OXFORD

SOT | Society of Toxicology
academic.oup.com/toxsci

TOXICOLOGICAL SCIENCES, 172(2), 2019, 417–434

doi: 10.1093/toxsci/kfz191
Advance Access Publication Date: August 19, 2019
Research Article

Perfluorooctane Sulfonate (PFOS) Produces Dopaminergic Neuropathology in *Caenorhabditis elegans*

Shreesh Raj Sammi,[*,†] Rachel M. Foguth,[*,†] Claudia Sofía Nieves,[*,†] Chloe De Perre,[‡] Peter Wipf,[§] Cynthia T. McMurray,[¶] Linda S. Lee,[‡] and Jason R. Cannon[*,†,1]

[*]School of Health Sciences; [†]Purdue Institute for Integrative Neurosciences; [‡]Department of Agronomy, Purdue University, West Lafayette, Indiana 47907; [§]Departments of Chemistry, Pharmaceutical Sciences, and Bioengineering, University of Pittsburgh, Pittsburgh, Pennsylvania 15260; and [¶]Molecular Biophysics and Integrated Bioimaging, Lawrence Berkeley National Laboratory, Berkeley, California 94720

[1]To whom correspondence should be addressed at Toxicology, 207 S. Martin Jischke Drive, West Lafayette, IN 47907. Fax: (765) 496-1377. E-mail: cannonjr@purdue.edu.

ABSTRACT

Perfluorooctane sulfonate (PFOS) has been widely utilized in numerous industries. Due to long environmental and biological half-lives, PFOS is a major public health concern. Although the literature suggests that PFOS may induce neurotoxicity, neurotoxic mechanisms, and neuropathology are poorly understood. Thus, the primary goal of this study was to determine if PFOS is selectively neurotoxic and potentially relevant to specific neurological diseases. Nematodes (*Caenorhabditis elegans*) were exposed to PFOS or related per- and polyfluoroalkyl substances (PFAS) for 72 h and tested for evidence of neuropathology through examination of cholinergic, dopaminergic, gamma-amino butyric acid (GABA)ergic, and serotoninergic neuronal morphologies. Dopaminergic and cholinergic functional analyses were assessed through 1-nonanol and Aldicarb assay. Mechanistic studies assessed total reactive oxygen species, superoxide ions, and mitochondrial content. Finally, therapeutic approaches were utilized to further examine pathogenic mechanisms. Dopaminergic neuropathology occurred at lower exposure levels (25 ppm, approximately 50 μM) than required to produce neuropathology in GABAergic, serotonergic, and cholinergic neurons (100 ppm, approximately 200 μM). Further, PFOS exposure led to dopamine-dependent functional deficits, without altering acetylcholine-dependent paralysis. Mitochondrial content was affected by PFOS at far lower exposure level than required to induce pathology (≥1 ppm, approximately 2 μM). Perfluorooctane sulfonate exposure also enhanced oxidative stress. Further, mutation in mitochondrial superoxide dismutase rendered animals more vulnerable. Neuroprotective approaches such as antioxidants, PFAS-protein dissociation, and targeted (mitochondrial) radical and electron scavenging were neuroprotective, suggesting specific mechanisms of action. In general, other tested PFAS were less neurotoxic. The primary impact is to prompt research into potential adverse outcomes related to PFAS-induced dopaminergic neurotoxicity in humans.

Key words: PFAS; PFOS; neurodegeneration; Parkinson's disease; GenX; PFOA.

Per- and polyfluoroalkyl substances (PFAS) are a group of compounds typically characterized by a hydrophobic carbon-fluorine tail and a nonfluorinated hydrophilic head. Because of the unique properties to repel oil and water, PFAS have been extensively used in industry, eg, in the manufacture of textiles, food packaging, carpets, upholstery, leather, waxes, adhesives,

paints, polishes, cosmetics, aviation hydraulic fluids, fire-fighting foams, and papers (Post *et al.*, 2012).

Perfluorooctane sulfonate (PFOS), perfluorooctanoic acid (PFOA), and other PFAS have been extensively used over the last 50 years in the United States until they were voluntarily phased out of production in 2002 for PFOS and initiated in 2006 for PFOA (USEPA, 2017). Of note, the USEPA has issued a drinking water advisory limiting PFOS levels to 70 parts per trillion (USEPA, 2019). However, the strength of the carbon-fluorine bond renders PFAS highly resistant to environmental and biological degradation (O'Hagan, 2008). Perfluorooctane sulfonate has an elimination half-life approximately 9 years in the human body (Larsen and Giovalle, 2015). Further, PFOS is still in use in many other countries. Measurements in animal tissue suggest that PFAS bioaccumulate (Chengelis *et al.*, 2009; Sanchez Garcia *et al.*, 2018). Thus PFAS, including PFOS will remain a public health concern for decades to come.

Animal PFAS studies have indicated potential risks such as tumors, neonatal death, and adverse outcomes in the hepatic, immune, and endocrine systems (epa.gov; Steenland *et al.*, 2010). With respect to neurological effects, PFAS (especially PFOS) have been shown to accumulate in the brains of large mammals and have been associated with alterations in neurotransmission (Dassuncao *et al.*, 2019; Eggers Pedersen *et al.*, 2015). In laboratory animals, PFOS toxicity studies suggest potential neurotoxicity. For example, PFAS-exposed neonatal mice exhibit alterations in the levels of proteins relevant to neuronal growth and synaptogenesis (Johansson *et al.*, 2009; Lee and Viberg, 2013). In motor specific tasks, developmentally PFOS-exposed male offspring exhibited significantly shorter latency to fall on the wire-hang test when they were 5–8 weeks old, suggesting a potential motor deficit (Onishchenko *et al.*, 2011). Studies in lower order systems also suggest alterations, where PFOS-treated *Caenorhabditis elegans* showed decreased motor function (Chen *et al.*, 2014). Finally, *in vitro* exposures suggest that PFAS may influence neuronal differentiation (Slotkin *et al.*, 2008). Taken together, there is a clear public health need to investigate PFAS-induced neurotoxicity and fill key gaps in our understanding of PFOS-induced neurotoxic mechanisms and neuropathology.

In the present study, we utilized *C. elegans* to test PFOS and PFOA neurotoxicity. *Caenorhabditis elegans* is a nonpathogenic nematode with features such as a short lifespan, transparent body, conserved neurotransmitters, and availability of transgenic and green fluorescent protein-based reporter strains for neuronal markers and various transcription factors (Ma *et al.*, 2018). Thus, this model system serves as a suitable intermediate between cell culture and higher order animal models (Hunt, 2017). The unique features of nematode models allowed us to test whether PFOS is selectively neurotoxic to specific neuronal populations, study mechanisms of neurotoxic action, and test potential therapeutic strategies across a wide range of dosing.

MATERIALS AND METHODS

Culture and maintenance of strains. *Caenorhabditis elegans* strains, Bristol N2, BZ555 (egls1[*dat-1p*::GFP]), CZ1632 (juIs76 [*unc-25p*::GFP + *lin-15*(+)]), GR1366 (mgIs42 [*tph-1*::GFP + rol-6(su1006)]), LX929 (vsIs48 [*unc-17*::GFP]), and *Escherichia coli* OP50, were procured from Caenorhabditis Genetics Centre, (University of Minnesota, Minnesota). VC433 (*sod-3*[gk235]) was provided by *C. elegans* Reverse Genetics Core Facility at University of British Columbia. *Caenorhabditis elegans* strains were grown on nematode growth medium (NGM) and cultured at 22°C. A synchronized population of worms was obtained by sodium hypochlorite treatment. Embryos were incubated overnight at 22°C to obtain L1-staged worms.

Table 1. Typical Exposure Level Range of Commonly Used Parkinson's Disease-Relevant Toxicants in *Caenorhabditis elegans*

Toxicant	Exposure Level Required to Induce Selective DA Neurodegeneration	Comments	References
Established Parkinson's disease-relevant models			
6-OHDA	10–50 mM	1-h exposure	Nass *et al.* (2002)
Manganese	50–150 mM	24-h exposure	Benedetto *et al.* (2010)
MPP+/MPTP	0.25–4 mM	24-, 48-, and 72-h exposure	Pu and Le (2008)
Paraquat	180 μM	24–96-h exposure	Gonzalez-Hunt *et al.* (2014)
Emerging Parkinson's disease models			
Harmane	100 μM	48-h exposure	Sammi *et al.* (2018)
PFOS[a]	Approximately 50 μM	72-h exposure	This report

PFOS elicits DA neurotoxicity at far lower exposure levels than most established Parkinson's disease-relevant neurotoxicants.
[a]For comparison, dosage here is reported in molarity. Throughout the remainder of the report, it is reported in ppm, a common unit for soil and groundwater contaminants.

PFAS treatments: overall dosage rationale. L1-stage worms were treated with different exposure levels of PFOS and PFOA (Sigma Aldrich, St Louis, Missouri) and cultured in liquid media as described (Stiernagle, 2006). Perfluorooctane sulfonate exposure levels were chosen from an extensive literature on the study of dopaminergic (DA) neurotoxicant in nematode models. In general, our exposure levels are below the levels of established DA neurotoxicants used in this model system (Table 1). The goal of this table is to place chosen PFOS concentration in the context of many nematode PD models. Here, it is worth noting that half-lives in liquid, bacteria, and in worms, along with absorption differences and other factors may influence toxicant-specific exposure level responses. The exposure levels selected were comparable to exposure levels detectable in human blood (0.004–1.656 ppm) (Olsen *et al.*, 2003) and animals (wood mice ranging from 0.47 to 178.55 ppm) (Hoff *et al.*, 2004). Previous studies in *C. elegans* have used exposure level up to 200 μM (approximately 100 ppm) (Xu *et al.*, 2016). Thus, exposure levels were somewhat higher than, but informed by environmental and biological levels.

Individual 10 000-ppm stocks of PFOS and PFOA were prepared in methanol and diluted further to exposure levels ranging from 1 to 200 ppm (for exposure level of 150 and 200 ppm, a 20 000 ppm stock was prepared). Fresh stocks <7-days old were used for each experiment and vortexed prior to use. A total of 70 L1-staged worms were added to a 200-μl suspension in 24-well plates and incubated at 22°C. The exposure level of methanol was adjusted accordingly for all the treatment groups including the control, so that the final exposure level would not exceed 1% (which was devoid of any neurodegenerative effect over the span of 72 h). Based on pilot experiments and the results obtained, most mechanistic studies were conducted at 75 ppm

(approximately 150 μM), whereas mitochondrial effects were measured as low as 1 ppm because pilot studies suggested heightened sensitivity of mitochondrial versus other endpoints.

Mechanistic studies using pharmacological agents. In order to identify the mechanisms of toxicity and test neuroprotective strategies, specific pharmacological agents such as DL-3-hydroxybutyric acid (HBA), N-acetyl-L-cysteine (NAC), glutathione (GSH), juglone (5-hydroxy-1,4-napthalenedione), XJB-5-131, buthionine sulfoximine (BSO) and β-cyclodextrin (BCD) were utilized. DL-3-Hydroxybutyric acid is known to confer neuroprotection through maintenance of succinate levels (complex I bypass) in the MPTP model of PD (Tieu *et al.*, 2003). DL-3-Hydroxybutyric acid is also reported to exhibit neuroprotection against *Streptomyces venezuelae* metabolite mediated DA cell loss (Ray *et al.*, 2014). N-acetyl-L-cysteine is a well-known antioxidant, a generalized activator of mitochondrial complexes I, IV, and V (Cocco *et al.*, 2005; Kamboj and Sandhir, 2011; Miquel *et al.*, 1995; Soiferman *et al.*, 2014) and a heavy metal chelator (Banner *et al.*, 1986). Besides, positive effects of NAC have also been demonstrated on lifespan in *C. elegans* (Oh *et al.*, 2015). XJB-5-131 is a hybrid molecule containing the β-turn region of gramicidin S and 4-amino Tempo (4-AT) and acts as a mitochondrial-targeted electron and reactive oxygen species (ROS) scavenger and superoxide dismutase mimetic, provide neuroprotection in Huntington disease models and rodent models of traumatic brain injury (Ji *et al.*, 2012; Khattab, 2006; Krainz *et al.*, 2016; Polyzos *et al.*, 2016; Xun *et al.*, 2012). The efficacy of XJB-5-131 was tested against both a known Parkinson's disease-relevant neurotoxicant that targets mitochondria (MPP^+) and PFOS (Pu and Le, 2008). MPP^+ studies and pilot PFOS studies using XJB-5-131 (10–100 μM) [final concentration of dimethyl sulfoxide (DMSO) being 1%] informed the final tested XJB-5-131 (12.5, 25, 50 μM) in PFOS-treated worms. Juglone is a known superoxide generator (Ishii *et al.*, 1990; Tawe *et al.*, 1998; Vanfleteren, 1993) and has been used to generate oxidative stress in *C. elegans* (Senchuk *et al.*, 2017). Glutathione is a natural antioxidant that has been reported to be affected in Parkinson's disease brains and plays an important role in disease pathogenesis (Martin and Teismann, 2009). Glutathione has been shown to confer neuroprotection in *C. elegans* (Martinez *et al.*, 2015). β-Cyclodextrin has been reported to dissociate binding of PFOA to human serum albumin (Weiss-Errico *et al.*, 2018). Thus, BCD was used as a cotreatment with PFOS to assess if it might also alter PFOS toxicity. β-Cyclodextrin has also been reported to internalize in *C. elegans* at adequately detectable levels (Lucio *et al.*, 2018).

For treatment with HBA, a 5 M stock of HBA sodium salt (Acros Organics, New Jersey, 150834), dissolved in sterile distilled water, was prepared. The worms were subjected to different exposure level (100, 150, and 200 mM) for 72 h in liquid culture. For treatment with NAC (Acros Organics, 160280250), a 500 mM stock was prepared in sterile distilled water. The worms were subjected to of 5, 10, and 15 mM of NAC (Oh *et al.*, 2015). For treatment with GSH, a 100 mM stock was prepared. Worms were treated with 0.125–2 mM GSH. For treatment with BCD, a 10 mM stock was prepared in distilled water and worms were treated with 150, 225, and 300 μM BCD. For treatment with XJB-5-131, 10 mM stocks were prepared in DMSO and worms were subjected to 12.5–50 μM XJB-5-131 (final concentration of DMSO being 0.5%), based on the outcome of pilot studies. For treatment with juglone, a 10 mM stock was prepared in 100% ethanol, which was diluted further to treat worms with 2.5 or 20 μM juglone (final concentration of ethanol ≤0.2%). Buthionine sulfoximine is a gamma glutamylcysteine synthetase inhibitor (Haddad, 2001) and has been used in *C. elegans* to study the effect of GSH biosynthesis on DA neurodegeneration (Martinez *et al.*, 2015). For treatment with BSO, a 10 mM stock solution of BSO was prepared in distilled water and worms were treated with the 50, 100, and 200 μM BSO.

Neurodegeneration assay. In order to determine the neuropathological effects of PFAS on specific neuron types, L1-staged worms expressing green fluorescence protein (GFP) in DA, gamma-amino butyric acid (GABA)ergic, serotonergic, and cholinergic neurons were subjected to different exposure level of PFOS (25–200 ppm) for 72 h at 22°C. Worms were identified using morphological markers of neurodegeneration that have been repeatedly utilized in nematode models by our group and others (Alexander *et al.*, 2014; Sammi *et al.*, 2018). The percentage of worms exhibiting neuropathological alterations, such as loss or breakage in dendrites, and loss of soma, was calculated. Any worm exhibiting above-mentioned neuropathological alterations in 1 or >1 neuron was counted as affected. This approach was particularly useful and simple, because neuronal subpopulations differ in number. Also, it was difficult to study individual neurons in dense network such as that made by cholinergic neurons. Thus, the overall approach was similar to our previous efforts and the prevailing literature, where we reported the percentage of worms exhibiting neurodegeneration of a specific neuronal subpopulation, whereas for DA neurons, we were also able to calculate a second measure, the percentage of neurons affected (Alexander *et al.*, 2014; Sammi *et al.*, 2018).

For a dense neuronal network such as cholinergic neurons, head neurons above the nerve ring were mainly considered for assessment. For other neuron types, ie, DA and serotonergic neurons, being less in number, it was generally feasible to count all visible neurons. Similarly, for (GABA)ergic neurons all neurons along with commissures were considered for the studies.

For in depth studies on dopaminergic neurons, neurodegeneration was quantified as described by Yao *et al.* (2010). Briefly, treated worms were washed 3 times using M9 buffer. Worms were anesthetized using 100 mM sodium azide and visualized using a fluorescence microscope (Olympus BX-53). Counting of neurons was done with respect to all neuron types, ie, Cepahlic sensila (CEP), Anterior deirid (ADE) and posterior deirid (PDE). The number of intact neurons was calculated for a minimum of 20 worms per group (independent replicates). Care was taken to keep the worm number constant and fresh stocks (no older than 1 week) of chemicals were used for all studies.

Estimation of internal levels of PFOS. For estimation of internal levels of PFOS, approximately 11 200 worms were treated with 0, 1, or 5 ppm of PFOS. After 72 h of incubation, worms were washed 3 times with M9 buffer. Worms were resuspended and washed on a rotary shaker for 1 h in 10 ml of M9 buffer. After 1 h, worms were centrifuged in preweighed centrifuge tubes. The worm pellet was then washed twice before flash freezing in liquid nitrogen. The supernatant was removed and wet weight for each pellet was calculated. Samples were stored at −80°C until use. Perfluorooctane sulfonate levels in representative samples were quantified by liquid chromatography with tandem mass spectrometry as detailed previously (Hoover *et al.*, 2017). Internal PFOS levels were normalized to wet weights as has been done in similar worm studies (Jonassen et al., 2001; Sanyal *et al.*, 2004). Bioconcentration factors (BCFs) were calculated as described (Gobas 2001: BCF = exposure level in tissue [ng/g wet

weight]/exposure level in medium [ng/ml]) representing the conservative estimates of bioexposure level factor.

Dihydroethidium staining. Dihydroethidium (DHE) staining for superoxide ions was performed in analogy to a literature protocol (Chikka *et al.*, 2016). Briefly, worms were washed 3 times with M9 buffer followed by 2 washes with phosphate buffered saline (PBS). About 50 worms suspended in 100 µl of PBS were mixed with an equal amount of 12 µM DHE (Millipore, Burlington, Massachusetts, 309800) dissolved in DMSO (stock concentration, 12 mM) and diluted in PBS (final exposure level of DMSO = 0.01%). After incubation in the dark for 40 min with intermittent agitation, worms were washed twice with PBS, anesthetized using 100 mM sodium azide and imaged using a fluorescence microscope (Olympus BX-53). A minimum of 20 animals per group were analyzed semiquantitatively using Image J (Schneider *et al.*, 2012) by drawing a region of interest (ROI).

Genetic cross to study the effect of sod-3 mutation on PFOS-mediated neurodegeneration. A genetic cross between BZ555 (dat-1_p::GFP) and VC433(*sod-3*(gk235)) was conducted as previously described (Pu and Le, 2008), with a slight modification. Briefly, BZ555 males (raised by heat-shock followed by crossing with BZ555 hermaphrodites) were crossed with VC433 hermaphrodites (in a 5:2 ratio of males to hermaphrodites, respectively). F-1 generation worms that showed GFP labeled DA neurons were picked and added to NGM–OP50 plates (35-mm plates). Self-fertilized progeny were further screened for positives (expressing GFP in DA neurons). Worms were picked from plates with 100% positive worms. In order to further validate the line, single worms were transferred to plates and genotyping (through single worm PCR) was conducted post egg laying for the transferred worms. Worms with homozygous deletions (designated as dat-1_p::GFP; *sod-3*(gk235)) were grown and used for the studies.

Quantitative estimation of ROS using H_2DCFDA. Reactive oxygen species estimation was conducted as described (Smita *et al.*, 2017), with a slight modification. Briefly, a 10 mM stock solution of H_2DCFDA in ethanol was further diluted to 100 µM using PBS. An equal number of worms were seeded in treatment plates (1000 per ml). On day 2, worms were washed using M9 buffer (3 times) and twice using PBS. An equal number of worms were added to each well of black 96-well plates. 150 µl of 100 µM H_2DCFDA was added to each well (150-µl worm suspension) to achieve a final concentration, 50 µM, and fluorescence was read every 60 min using a Molecular devices Spectramax M2 for 180 min (excitation/emission: 485/520). Readings were normalized with respect to the control. For ROS estimation in galactose-supplemented SH-SY5Y cells, a confluent population of galactose-supplemented SH-SY5Y cells (approximately 15 000) were treated with PFOS (25–200 ppm) for 24 h. Post treatment, cells were incubated for 6 h with H_2DCFDA (1 µM). Fluorescence was read using Molecular devices Spectramax M2. Data were normalized with respect to control.

Mitochondrial stress test in SHSY-5Y cells. A mitochondrial stress test was conducted using the Seahorse Bioscience XFp analyzer in galactose-supplemented SH-SY5Y cells as per the manufacturer's protocol. Briefly, SH-SY5Y cells were cultured in galactose media prepared by dissolving glucose-free RPMI1640 (7.2 g l^{-1}), sodium pyruvate (1 mM), and sodium bicarbonate (44 mM) in 810 ml of distilled water. The pH was adjusted to 7.2 using 1 M hydrochloric acid and the media was further supplemented with 10 ml of 100× L-glutamine, 9 ml of 20% galactose, 10 ml of 1 M HEPES, 10 ml of penicillin-streptomycin, and 150 ml of Nu Serum growth supplement. The media was filtered and stored at 4°C. A total of 35 000 cells were plated in each well (B–G) of Seahorse XFp cell culture miniplates and incubated for 24 h at 37°C with 5% carbon dioxide. Wells A and H were used without cells as background. Cells were treated with 75 ppm PFOS (within a range commonly used to evaluate DA neurotoxicants [Li *et al.*, 2015]) and incubated for another 24 h. Sensor cartridges were prepared with distilled water and incubated overnight at 37°C. Post 24 h, cells were incubated with 155 µl basic media (Seahorse basic media [14.5 ml], 20% galactose [10 mM], 100× L-glutamine [3.77 mM], and sodium pyruvate [1 mM] at 37°C for 1 h). Meanwhile, XFp calibrant was added to the sensor plates and incubated at 37°C for 30 min. Oligomycin (8 µM), Carboxyl Cyanide-4-(trifluoromethoxy) phenylhyrazone (4.5 µM), and antimycin A/rotenone mixture (10 µM) was added to port A, B, and C, respectively, and the sensor plate was loaded in the machine. After calibration, the culture miniplate was inserted into the machine and the mito stress test was run. Data were analyzed using the cell mito stress test report generator.

MitoTracker staining and quantification. MitoTracker staining was performed as described (Gaffney *et al.*, 2014), with a slight modification. Briefly, MitoTracker Red CM-H2XRos was added to liquid culture on day 2 and mixed gently. MitoTracker Red stock solution was prepared by dissolving 50 µg MitoTracker Red CM-H_2XRos in 100 µl of DMSO. MitoTracker Red (final concentration, 4.72 µM) was fed to worms by mixing it with *E. coli* OP50. Worms were washed off using M9 buffer on day 3, incubated with *E. coli* OP50 solution for 30 min and washed again 3 times using M9 buffer. Worms were anesthetized using 100 mM sodium azide and observed under a fluorescence microscope (Olympus BX-53). Approximately 20 worms per group were analyzed semiquantitatively using Image J (Schneider *et al.*, 2012). The gut region was excluded from ROI analysis, in order to eliminate nonspecific fluorescence.

1-Nonanol assay. In order to evaluate dopamine-dependent motor behavior (as an indirect measure of dopamine levels), 1-nonanol based repulsive behavior (Bargmann *et al.*, 1993) was quantified. The relationship between dopamine levels and repulsion time has been repeatedly shown in the literature. Worms with optimum levels of dopamine exhibit repulsive behavior when exposed to 1-nonanol, whereas worms with lower levels of dopamine require prolonged time to show the repulsive behavior; increases in dopamine, correspondingly decrease 1-nonanol repulsion time (Sammi *et al.*, 2018; Smita *et al.*, 2017). The 1-nonanol repulsion assay for indirect quantification of dopamine levels was performed as previously described (Sammi *et al.*, 2018). Briefly, treated worms were washed 3 times with M9 buffer. Worms were placed on NGM plates. The poking lash dipped in 1-nonanol (Acros Organics, AC157471000) was placed close to the head region of the worms while taking care not to touch the worms. Care was also taken not to over immerse the poking lash in 1-nonanol because excess 1-nonanol on the agar plate comes in contact with the worms while also desensitizing them due to prolonged exposure. Any worm prodded accidentally was disregarded in order to rule out the interference from the mechanosensory stimulus. Time taken for the worms to show repulsive behavior was counted using a stop watch. Stop watch was started as the poking lash was placed close to head region and stopped when worm reversed and turned head ≥45°. Previous studies in worms have validated the assay by exposing

the worms to DAT inhibitor, bupropion HCl, and simultaneously conducting the assay in worms overexpressing *cat-2* (encodes tyrosine hydroxylase) and *cat-2* mutants (Sammi *et al.*, 2018). Additionally, RNAi of *cat-2* has also been shown to enhance repulsion time in worms (Kaur *et al.*, 2012). Furthermore, *cat-2* mutants have also shown increased repulsion time in response to octanol with reversal in presence of exogenous dopamine (Baidya *et al.*, 2014).

Acetylcholine-dependent paralysis (Aldicarb) assay. Determination of acetylcholine based function was conducted as described (Mahoney *et al.*, 2006). Briefly, treated worms were washed 3 times and were transferred to NGM-Aldicarb plates (0.5 mM Aldicarb). Aldicarb is an acetylcholinesterase inhibitor and exposure leads to accumulation of acetylcholine, resulting in flexion of muscles. The percentage of worms paralyzed at a time point is proportional to acetylcholine levels. The number of paralyzed worms was counted every 30 min. Any worms lost or injured were not considered as the part of study. The percentage of worms paralyzed was calculated when approximately 50% of worms were paralyzed in the control group. The Aldicarb assay has been successfully utilized to study functional alterations resulting from perturbed synaptic transmission (Mahoney *et al.*, 2006). Previous studies have indicated its efficacy in determining the effect on cholinergic transmission in phytomolecules and established pharmacological AcHE inhibitors such as donepzil (Mulcahy *et al.*, 2013; Sammi *et al.*, 2017).

Statistical analysis. Statistical analysis was performed using GraphPad PRISM, Version 7.02 (1992–2016 GraphPad Software, Inc, La Jolla, California). Each experiment was repeated at least 3 times and normalized to untreated groups. Data are expressed as mean ± S.E.M. Analysis of variance (ANOVA), followed by Dunnett's (where comparison was only to control) and Sidak's (in case of two-way ANOVA) post hoc tests were utilized. For all experiments, $p < .05$ was deemed statistically significant.

RESULTS

Heightened DA Neuron Vulnerability to PFOS

In view of the lack of information on PFOS neurotoxicity, we determined the effect of PFOS on different neuron types (Figure 1). Green fluorescence protein reporter strains specific to neuron types such as DA (BZ555), GABA (CZ1632), serotonin (GR1366), and acetylcholine (LX929) were exposed to PFOS within the range 25–200 ppm (equivalent to 50–400 μM) for 72 h. Dopaminergic neurodegeneration in nematodes is typically quantified through the percentage of worms exhibiting neurodegeneration or the percentage of individual neurons exhibiting neurodegeneration. Here, we have quantified both indices (Figs. 1 and 2) similar to our previous report that studied a different chemical class (Sammi *et al.*, 2018).

Dopaminergic neurons were found to be more vulnerable, exhibiting a significant decrease in the percentage of worms lacking neurodegeneration at 25 ppm (78.33 ± 1.667, $p = .0343$), 50 ppm (73.33 ± 8.33, $p = .0088$), 75 ppm (56.66 ± 6.00, $p = .0001$), 100 ppm (50.00 ± 7.63, $p = .0001$), 150 ppm (8.33 ± 1.66, $p = .0001$), and 200 ppm (0.00 ± 0.00, $p = .0001$; $n = 3$) (Figs. 1A and 1B). The IC50 value for PFOS in BZ555 was found to be 160 μM.

Comparatively, GABAergic, serotonergic and cholinergic neurons were less sensitive than DA neurons, requiring higher PFOS concentration. These subpopulations exhibited a significant decrease in the percentage of worms lacking neurodegeneration only at 100 ppm and above. GABAergic neurons exhibited a decrease in the percentage of worms lacking neurodegeneration at 100 ppm (83.33 ± 1.66, $p = .0005$), 150 ppm (83.33 ± 3.33, $p = .0005$), and 200 ppm (53.33 ± 4.41, $p = .0001$; $n = 3$) (Figs. 1C and 1D). The IC50 value for PFOS in GR1366 was found to be 283.3 μM.

Similarly, serotonergic neurons exhibited a decrease in the percentage of worms lacking neuronal damage at 100 ppm (75.00 ± 0.00, $p = .0001$), 150 ppm (55.00 ± 5.00, $p = .0001$), and 200 ppm (48.33 ± 3.33, $p = .0001$; $n = 3$) (Figs. 1E and 1F). The IC50 value for PFOS in GR1366 was found to be 203.8 μM.

Cholinergic neurons also followed the same trend, exhibiting a decrease in the percentage of worms lacking neurodegeneration at 100 ppm (85.00 ± 0.00, $p = .0003$), 150 ppm (85.00 ± 2.87, $p = .0003$), and 200 ppm (83.33 ± 1.66, $p = .0001$; $n = 3$) (Figs. 1G and 1H).

After identifying enhanced sensitivity of DA neurons to PFOS, we studied the concentration and time-dependent effect of PFOS on DA neurons. A significant decrease in the percentage of intact neurons was observed at 75 ppm (78.33 ± 0.41, $p = .0023$), 100 ppm (69.16 ± 4.15, $p = .0001$), 150 ppm (34.37 ± 5.31, $p = .0001$), and 200 ppm (21.04 ± 1.50, $p = .0001$; $n = 3$) (Figs. 2A and 2B).

Time course studies were conducted at 2 exposure levels, 75 and 100 ppm for 3 time points, 24, 48, and 72 h. In worms treated with 75 ppm PFOS, a significant decrease in the percentage of total intact neurons was observed at 48 h (82.29 ± 4.79, $p = .0183$) and 72 h (57.91 ± 4.35, $p = .0001$) (Figure 2C).

At higher concentration (100 ppm), the effect was more pronounced, where a larger reduction in the percentage of intact neurons at 48 h (60.20 ± 2.20, $p = .0001$) and 72 h (60.20 ± 2.20, $p = .0001$) was observed (Figure 2D). Perfluorooctane sulfonate also produced developmental delay, which was more pronounced at higher doses and therefore higher doses (100 and 200 ppm) were not utilized for mechanistic studies. Unlike PFOS, GenX and PFOA did not produced detectable developmental delay.

PFOS Accumulation in C. elegans

Internal PFOS levels in worms (on a wet weight basis) increased in relation to applied PFOS (0–5 ppm) with 0.06 ± 0.02 ppm at 0 ppm (controls), 13.06 ± 3.61 at 1 ppm and 52.02 ± 17.22 ($p = .0197$ vs control) at 5 ppm (Figure 3A). Up to 13-fold, BCF was observed with BCFs of 13.01 ± 3.61 and 10.40 ± 3.44 calculated for 1 and 5 ppm, respectively (Figure 3B).

PFOS Significantly Reduces Dopamine-Dependent Function Without Altering Acetylcholine-Dependent Function

Caenorhabditis elegans treated with PFOS (1–75 ppm) exhibited a significant increase in repulsion time at 25 ppm (3.43 ± 0.21, $p = .0002$), 50 ppm (3.86 ± 0.15, $p = .0001$), and 75 ppm (4.30 ± 0.21, $p = .0001$) in comparison to optimum levels in the untreated control (1.71 ± 0.007; $n = 3$) (Figure 4A), implying that PFOS reduces dopamine levels in a concentration-dependent manner.

In contrast, PFOS-treated worms did not exhibit any significant alterations in the Aldicarb assay (Figure 4B). Overall, these results indicate that PFOS (within the range 1–75 ppm) specifically alters dopamine levels, whereas Ach levels remain unaffected.

PFOS-Induced Alterations in ROS

Oxidative stress is known to play critical role in DA cell loss in PD (Dias *et al.*, 2013). Here, we quantified both ROS levels and, specifically, superoxide levels using H_2DCFDA and DHE staining,

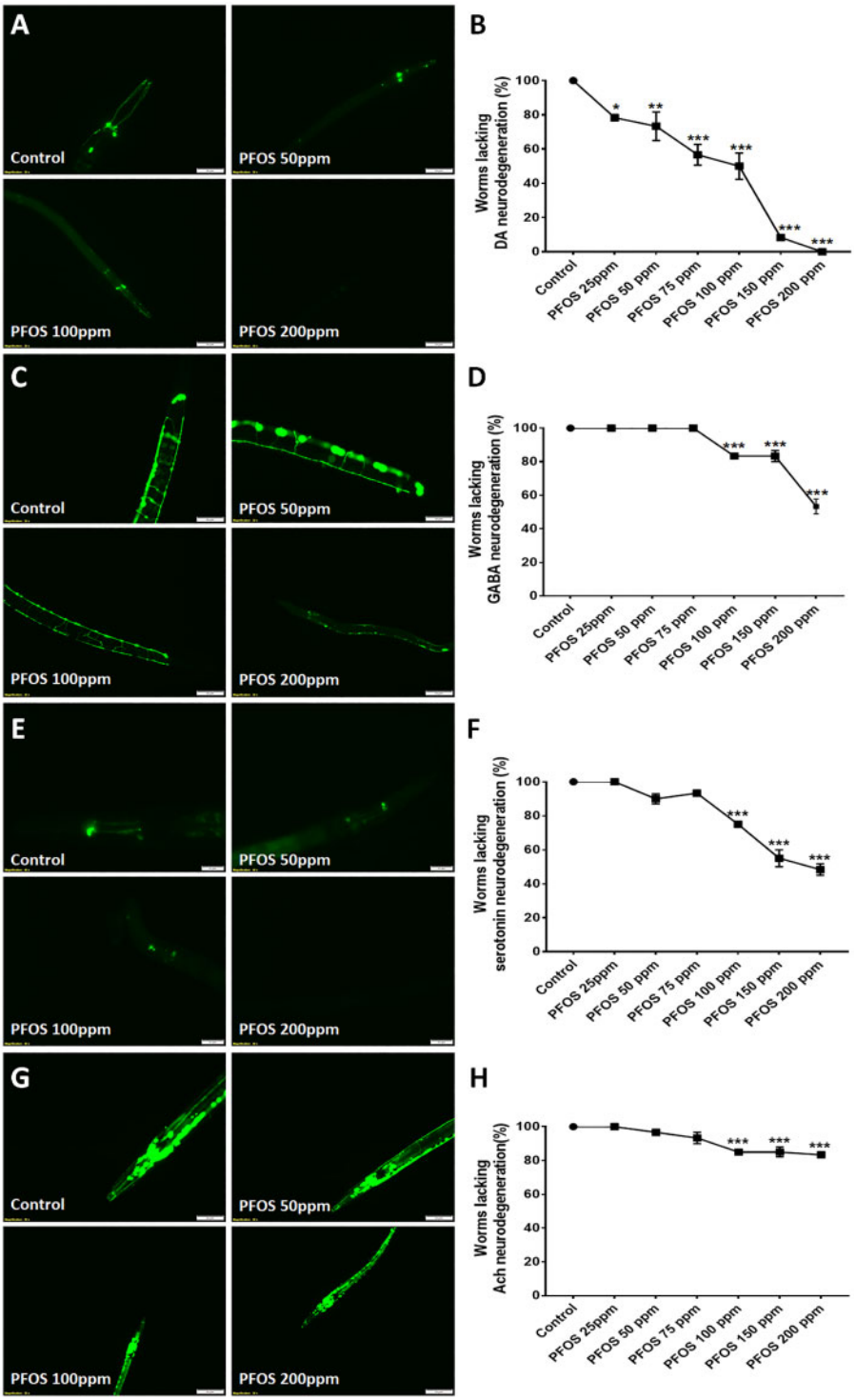

Figure 1. Dopaminergic (DA) neurons are selectively sensitive to perfluorooctane sulfonate (PFOS) exposure; an effect that is exposure level and time dependent. Worms (Strain: BZ555) were treated with PFOS (exposure level range: 25–200 ppm) for 72 h and neurodegeneration was assessed. Dopaminergic neurons exhibited heightened sensitivity to PFOS, with neurodegeneration observed at exposure levels as low as 25 ppm ($n = 3$) (A, B). Other neuron types, gamma-amino butyric acid (GABA)ergic (Strain: CZ1632) (C, D), serotonergic (Strain: GR1366) (E, F), and cholinergic (Strain: LX929) (G, H) were comparatively less susceptible to PFOS-induced neurodegeneration, exhibiting neuron loss at 100 ppm and above, when exposed to PFOS for 72 h. Data are presented as mean ± S.E.M. Percent of worms lacking neuronal damage was calculated by counting the number of worms with afflicted neurons for 20 animals in each experimental group. Data were analyzed using one-way analysis of variance (ANOVA) followed by Dunnett's post hoc test. $^{*}p < .05$, $^{**}p < .005$, and $^{***}p < .001$ ($n = 3$). Scale bar represents 50 μM (A, C, G) and 20 μM (E).

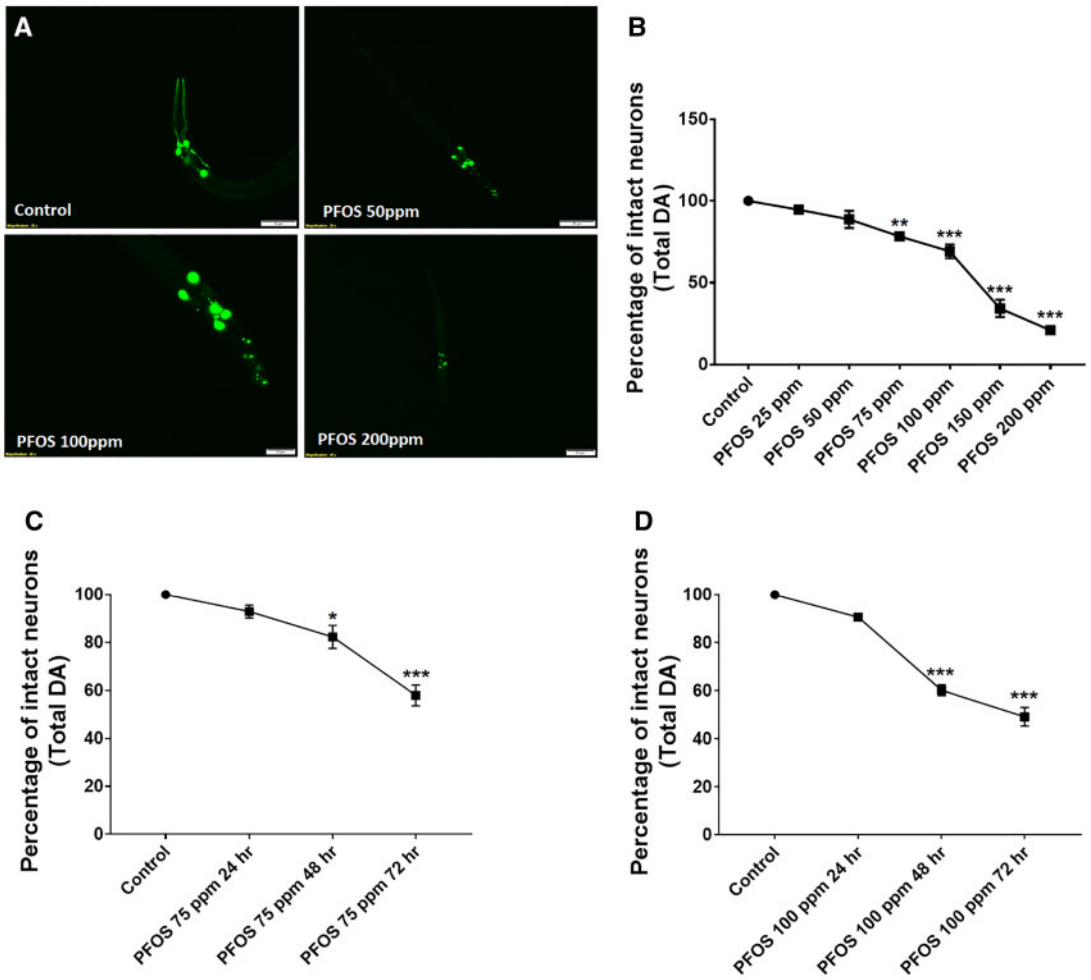

Figure 2. PFOS treatment causes DA cell loss that is concentration and time dependent. Treatment of worms with PFOS (exposure level range: 25–200 ppm for 72 h) resulted in distinct morphological changes such as axon breaks or loss of dendrites, swelling, and loss of soma, representative of neuronal damage in worms (A). The percentage of neuronal loss calculated with respect to total neurons (B). Time course studies at 75 ppm (C) and 100 ppm (D) exhibited a significant impact of exposure time on DA cell loss in worms. Data are presented as mean ± S.E.M. The percentage of intact neurons was calculated by counting the total number of neurons in each worm for 20 worms per experimental group. Data were analyzed using one-way ANOVA followed by Dunnett's post hoc test. $^{*}p < .05$, $^{**}p < .005$, and $^{***}p < .001$ ($n = 3$). Scale bar represents 50 μM (A; Control and 50 ppm PFOS) and 20 μM (PFOS 100 and 200 ppm).

respectively. H_2DCFDA, which is a generalized ROS specific probe that detects hydroxyl, nitric oxide, and carbonate anion radicals (Kalyanaraman *et al.*, 2012) exhibited a significant increase at 50 ppm (1.82 ± 0.36, $p = .0259$), 75 ppm (1.75 ± 0.20, $p = .0456$), 100 ppm (2.08 ± 0.16, $p = .0022$), and 200 ppm (2.05 ± 0.06, $p = .0030$; $n = 3$) (Figure 5A).

Prior reports linked enhanced superoxide dismutase activity in response to PFOS exposure in SH-SY5Y cells (Chen *et al.*, 2014), Hep G2 cells (Hu and Hu, 2009), and fish (Liu *et al.*, 2007). We observed a significant decrease in superoxide levels (normalized to control), evident through DHE staining at 5 ppm (0.57 ± 0.00, $p = .0001$) and 25 ppm (0.17 ± 0.01, $p = .0001$) in comparison to control. A marginal upshift in superoxide ions was observed at higher exposure levels: 50 ppm (0.17 ± 0.01, $p = .0001$), 75 ppm (0.30 ± 0.04, $p = .0001$), 100 ppm (4.30 ± 0.21, $p = .0001$), and 200 ppm (0.49 ± 0.04, $p = .0001$; $n = 3$) (Figs. 5B and 5C).

PFOS-Mediated Neurodegeneration: Independence From Superoxide Levels

Due to the observed reduction in superoxide ions, we wanted to identify whether there is a correlation between superoxide levels and neurodegeneration. We used low exposure levels of superoxide generator, juglone (5-hydroxy-1, 4-napthalenedione) (Ishii *et al.*, 1990; Tawe *et al.*, 1998; Vanfleteren, 1993) to determine whether increasing superoxide levels could affect neuronal lesions. Prior to cotreatment with PFOS and juglone, we determined the effective, nonneurotoxic concentration of juglone through assessment of different exposure levels for superoxide radical generation (DHE staining), total ROS (H_2DCFDA), and neurodegeneration assay. We observed a significant increase in superoxide radicals in worms treated with 5 μM (1.57 ± 0.02, $p = .000$), 10 μM (1.89 ± 0.03, $p = .000$), and 20 μM juglone (2.46 ± 0.13, $p = .000$; $n = 3$) in comparison to untreated control (Figs. 5D and 5E). Juglone also exhibited significant increase in ROS levels at 5 μM (2.18 ± 0.37, $p = .009$) and 10 μM (2.98 ± 0.33, $p = .000$; $n = 3$) in comparison to control (Figure 5F). Further, we observed that higher exposure levels of juglone (ie, 20 μM) were toxic to DA neurons, exhibiting reduction in percentage of intact neurons being (81.66 ± 2.70, $p = .000$; $n = 3$) (Figure 5G). Hence, further studies to determine if superoxide radicals can alter PFOS-mediated neurodegeneration, lower exposure levels of juglone supplementation (2.5 μM and 5 μM) were chosen. Cotreatment with juglone was devoid of any significant alteration in PFOS-mediated DA cell loss (Figure 5H).

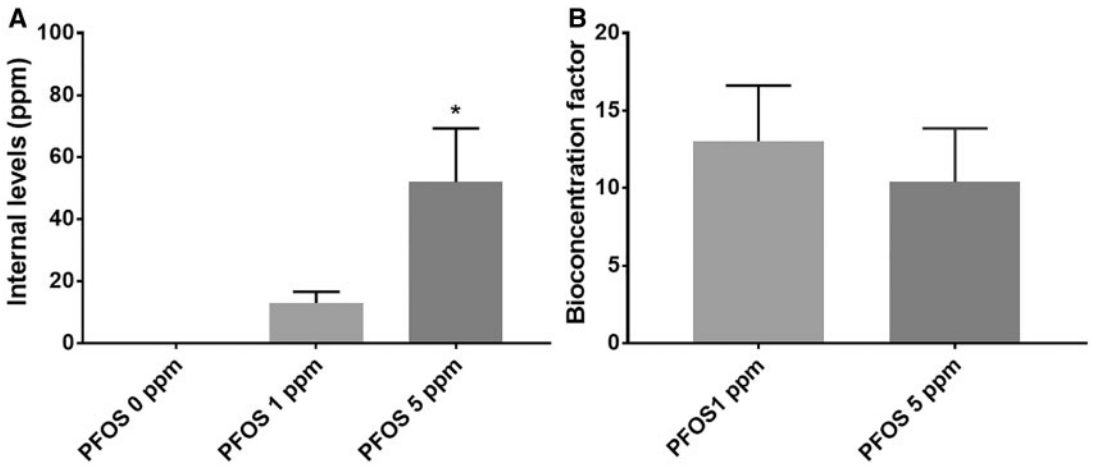

Figure 3. Internal PFOS levels and bioaccumulation. PFOS treatment at exposure levels (0, 1, and 5 ppm) for 72 h produced bioaccumulation in terms of quantified internal levels (A) and calculated bioconcentration factor (B). Data are presented as mean ± S.E.M. Data were analyzed using one-way ANOVA followed by Dunnett's post hoc test. $^{*}p < .05$ ($n = 3$).

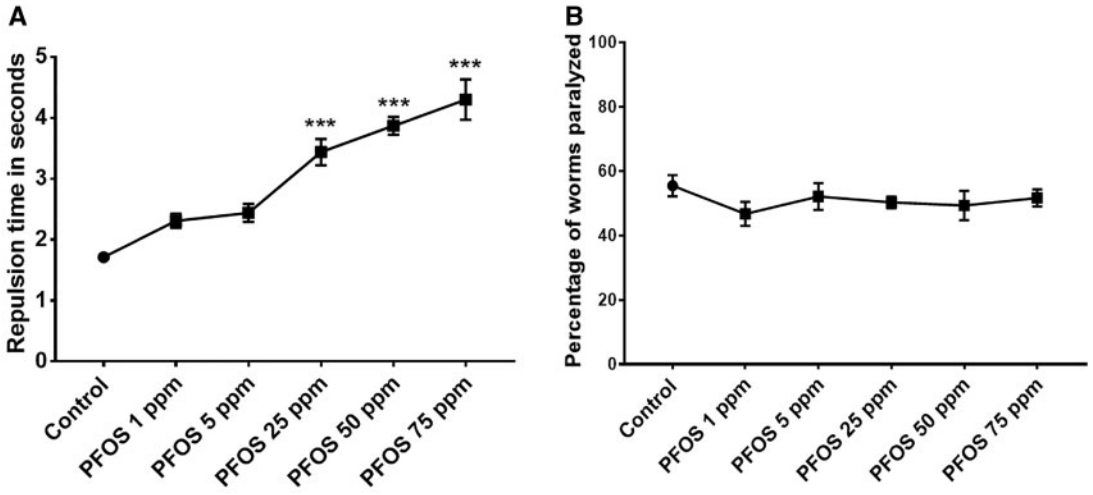

Figure 4. PFOS selectively affects dopamine-dependent behavior. PFOS treatment altered dopamine-dependent behavior at exposure levels of 25, 50, and 75 ppm for 72 h, as evident from significant delay in repulsion time in response to 1-nonanol (A). Acetylcholine-dependent function was not affected at tested exposure levels (1–75 ppm) (B). Data are presented as mean ± S.E.M. Repulsion time was calculated for 20 animals per experimental group. The percentage of worms paralyzed was scored for approximately 30–40 worms at the time point when about 50% of the worms were paralyzed in the control. Data are presented as mean ± S.E.M. Data were analyzed using one-way ANOVA followed by Dunnett's post hoc test. $^{***}p < .001$ ($n = 3$).

Furthermore, we also employed mutants for mitochondrial SOD (*sod-3*(gk235)) to ascertain if curtailed SOD activity in mitochondria alters effects of PFOS (50–100 ppm). We observed that not only were *sod-3* mutants, more vulnerable to the deleterious effects of PFOS (Figure 5J), but they also exhibited significant developmental delays in comparison to normal, worms (Figure 5I). A significant decrease in the percentage of intact neurons was observed at 50 ppm for BZ555 (90.00 ± 1.44) versus *sod-3* mutants (57.91 ± 1.98, $p < .0001$), 75 ppm for BZ555 (65.20 ± 4.48) versus *sod-3* mutants (24.37 ± 1.30, $p = .0001$), and 100 ppm for BZ555 (55.83 ± 3.50) versus *sod-3* mutants (40.00 ± 2.25, $p = .0009$; $n = 3$) (Figure 5K). The above results imply that decreased superoxide ions were unrelated to PFOS-mediated neurodegeneration, whereas mutation in mitochondrial superoxide dismutase renders DA neurons more vulnerable to PFOS.

PFOS-Induced Alterations in Mitochondrial Content and Function

Dysfunctional mitochondria are one of the critical hallmarks in Parkinson's disease (Park *et al.*, 2018) and Parkinson's disease-relevant toxicants, such as rotenone target mitochondria (Chernivec *et al.*, 2018; Greenamyre *et al.*, 2003). We studied the effect of PFOS on mitochondrial content in nematodes using reduced MitoTracker red staining. We observed a significant reduction in mitochondrial content at exposure levels as low as 1 ppm (0.65 ± 0.05, $p = .0001$) with further decreases at higher exposure levels of 5 ppm (0.40 ± 0.03, $p = .0001$), 10 ppm (0.19 ± 0.02, $p = .0001$), 25 ppm (0.17 ± 0.00, $p = .0001$), 50 ppm (0.07 ± 0.00, $p = .0001$), and 75 ppm (0.05 ± 0.00, $p = .0001$) (Figs. 6A and 6B). We also assessed the effect of PFOS on ROS levels in galactose-supplemented SH-SY5Y cells using H_2DCFDA. We observed a significant elevation in ROS levels at 25 μM (1.94 ± 0.08, $p = .000$), 50 μM (2.33 ± 0.12, $p = .000$), 75 μM (2.35 ± 0.18, $p = .000$), 100 μM (2.44 ± 0.11, $p = .000$), and 200 μM (2.47 ± 0.08, $p = .000$, $n = 3$) (Figure 6C).

To assess mitochondrial function, we conducted cellular mito stress tests in SH-SY5Y cells treated with 75-ppm PFOS. We observed a significant decrease in the oxygen consumption rate (oxidative phosphorylation) (Figure 6D) and extracellular

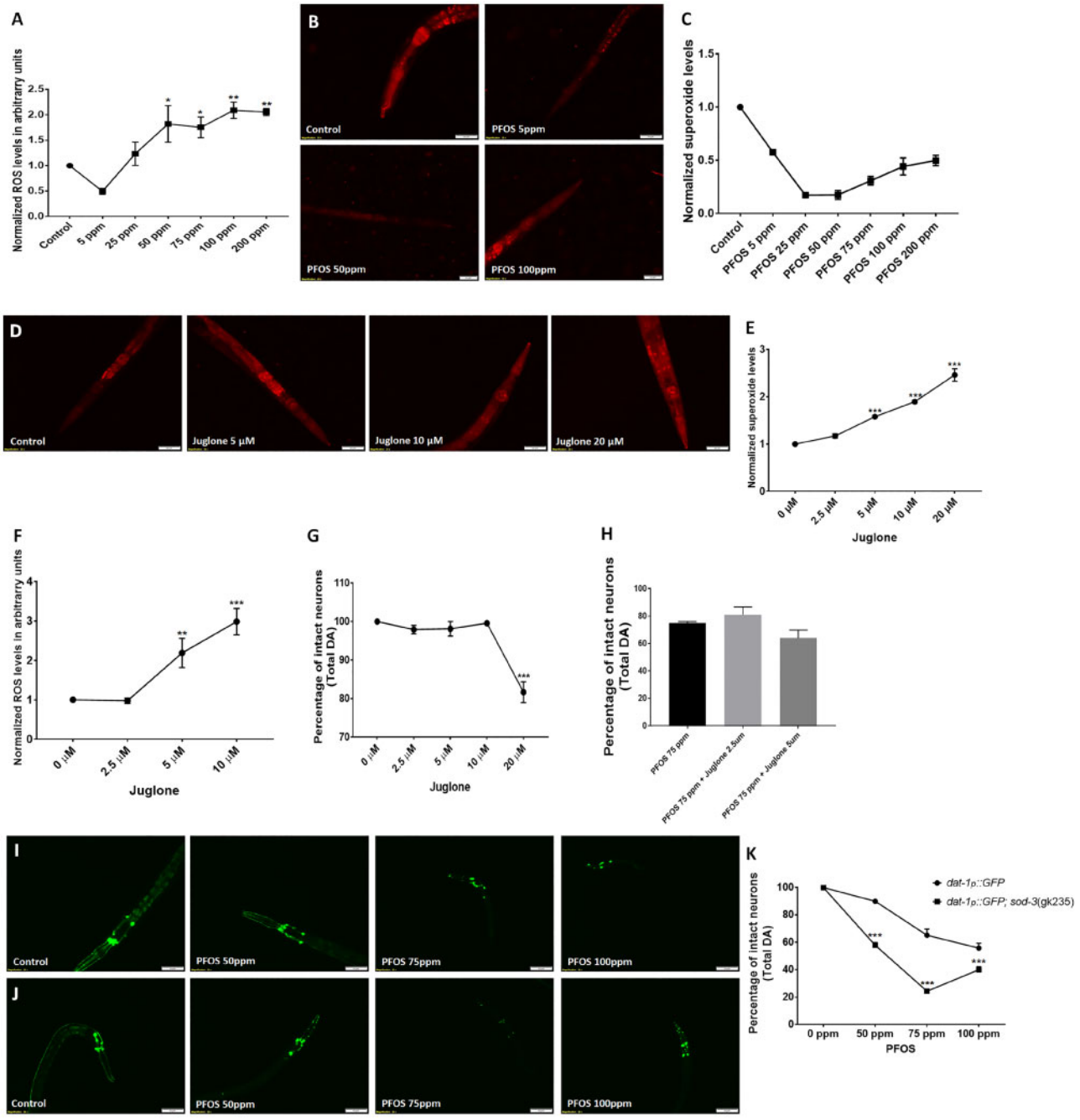

Figure 5. PFOS treatment altered levels of superoxide radicals and reactive oxygen species (ROS); DA cell loss was independent of superoxide radicals. Total ROS levels (normalized to control) measured using H_2DCFDA, exhibited a concentration-dependent increase (A). Worms treated with PFOS exhibited a reduction in superoxide levels (normalized to control) at lower exposure levels (5–50 ppm) which exhibited a gradual upshift at higher exposure levels (75–200 ppm) (B, C). Juglone, a superoxide generator showed exposure level-dependent increase in superoxide levels (D, E) along with significant increase in ROS levels at 5 and 10 µM (F). Worms were devoid of DA cell loss within the range 2.5–5 µM of juglone (G). Cotreatment with the juglone did not seem to affect DA cell loss (H). Mutants for mitochondrial SOD (*sod-3*(gk235)) exhibited elevated cell loss (J) in comparison to BZ555 worms (I), when treated with PFOS (50, 75, and 100 ppm) (K). Treatments conducted for a duration of 72 h. Data are presented as mean ± S.E.M. Data were analyzed by two-way ANOVA (K) followed by Sidak's post hoc test for grouped analysis and by one-way ANOVA followed by Dunnett's post hoc test. $^{*}p < .05$, $^{**}p < .01$, and $^{***}p < .001$ ($n = 3$). Scale bar represents 20 µm (A) and 50 µm (E, F).

acidification rate (Figure 6E), proton leak (0.60 ± 0.04, $p = .0009$) (Figure 6F), and nonmitochondrial oxygen consumption (0.38 ± 0.04, $p = .0002$) (Figure 6G) in comparison to normalized values of control. However, there were no significant changes in ATP production (Figure 6H).

Neuroprotective Efficacy of Antioxidant Treatments

MPP^+ served as a positive for Parkinson-disease-relevant mitochondrial toxicant because it is utilized to model Parkinson's disease in *C. elegans* (Pu and Le, 2008). Worms cotreated with 1.5 mM, MPP^+, and 10 µM XJB-5-131, (74.74 ± 8.11, $p = .0059$),

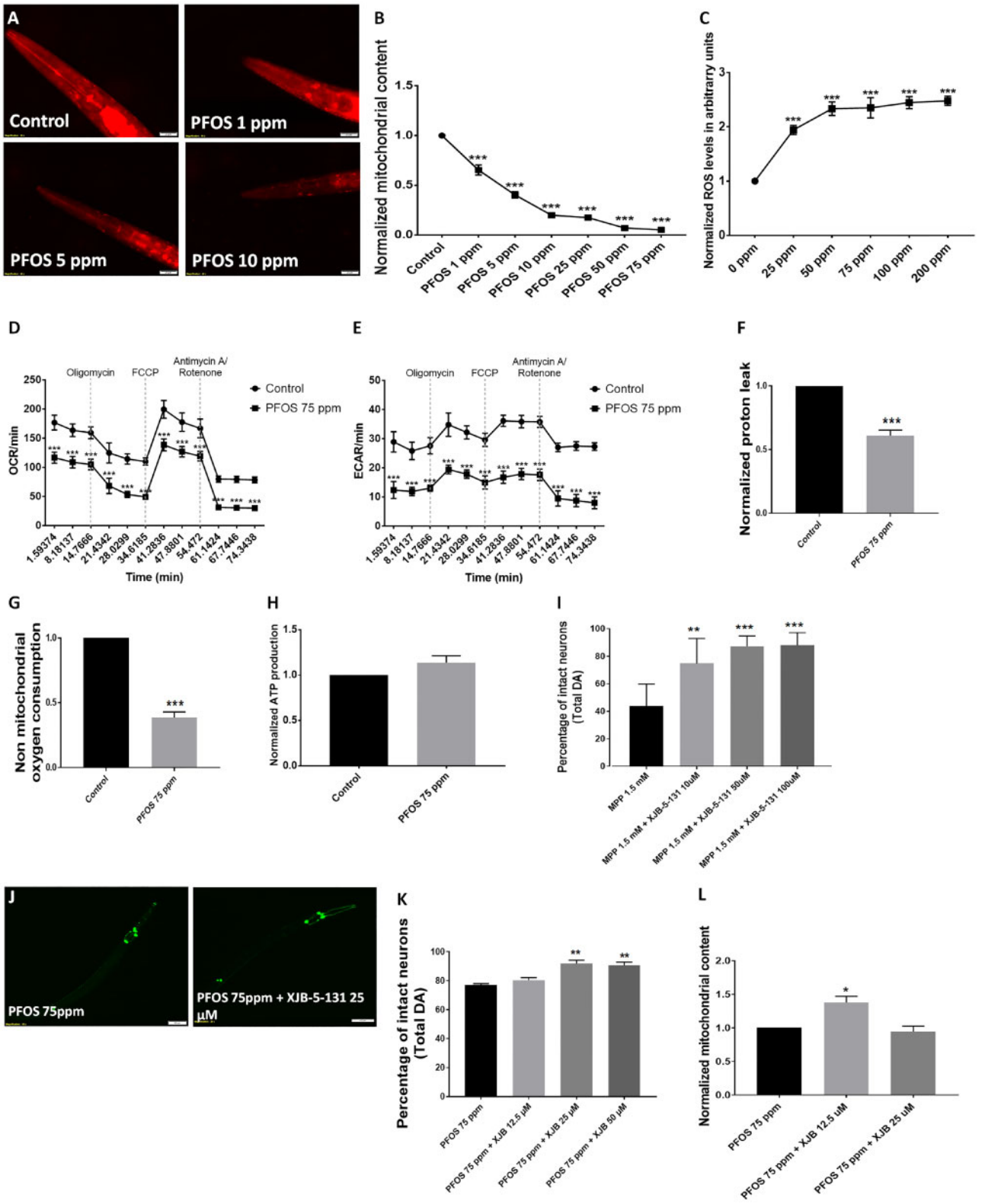

Figure 6. PFOS affects mitochondrial content and the mitochondrial-targeted radical and electron scavenger XJB-5-131 provides modest neuroprotection. PFOS treatment produced a loss of mitochondrial content in nematodes (A). Statistically significant decreases in mitochondrial content was observed at exposure 1 ppm and above in worms treated for 72 h. (B). PFOS led to significant elevation in ROS levels in galactose-supplemented SH-SY5Y cells, detected using H_2DCFDA (C). In PFOS-treated galactose-supplemented SH-SY5Y cells, the oxygen consumption rate as a marker of oxidative phosphorylation and extracellular acidification rate as a marker of glycolysis was reduced (D, E). Cells treated with PFOS exhibited a decrease in proton leak (D) and nonmitochondrial oxygen consumption (E), whereas alteration in ATP production was insignificant (H). Use of the targeted radical and electron scavenger, XJB-5-131, significantly rescued cell loss in worms challenged with MPP^+ (I). XJB-5-131 partially rescued cell loss in worms treated with PFOS (J). The percentage of neuronal loss scored with respect to total neurons for cotreatment with XJB-5-131 was rescued (K). XJB-5-131 also exhibited partial alleviation of mitochondrial content in worms challenged with PFOS (L). Treatments conducted for a duration of 24 and 72 h in cells and worms, respectively. Data are presented as mean ± S.E.M. Data were analyzed using one-way ANOVA followed by Dunnett's post hoc test. $^{**}p < .005$ and $^{***}p < .001$ ($n = 3$). Scale bar represents 20 µm (A) and 50 µm (F).

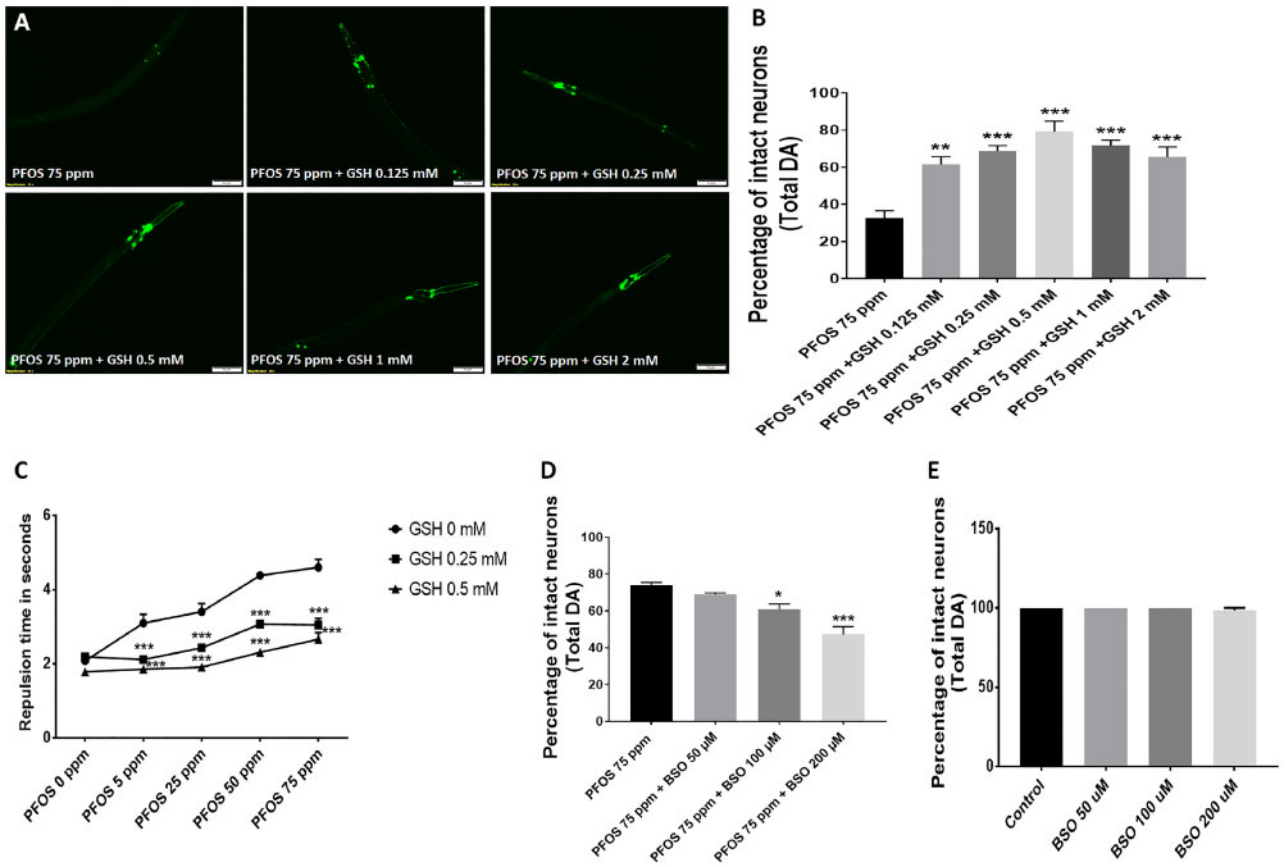

Figure 7. Glutathione (GSH) treatment reduces PFOS-induced DA neurodegeneration. The neuroprotective effects of GSH were evaluated for supplementation in polyfluoroalkyl substance (PFAS)-treated worms (75 ppm) (A). Worms cotreated with GSH exhibited decreased DA cell loss (B). Worms treated with GSH also exhibited protection from PFAS-induced functional deficits as quantified through the dopamine-dependent 1-nonanol repulsion assay (C). Cotreatment with buthionine sulfoximine (BSO), a gamma glutamylcysteine synthetase inhibitor, exhibited decrease in percentage of intact DA cells (D); exposure level of BSO employed (50–200 μM) did not exhibit neurotoxicity to DA neurons in untreated worms (E). Treatments conducted for a duration of 72 h. Data are presented as mean ± S.E.M. Data were analyzed by one-way ANOVA (B) or by two-way ANOVA (C) for grouped analysis and followed by Dunnett's post hoc test. $^{**}p < .01$ and $^{***}p < .001$ ($n = 3$). Scale bar represents 50 μm.

50 μM XJB-5-131, (87.24 ± 3.36, $p = .0003$), and 100 μM XJB-5-131 (88.09 ± 4.03, $p = .0003$) exhibited an increase in the number of intact neurons in comparison to worms treated with MPP^+ (43.65 ± 7.21) (Figure 6I). Because our data show elevated ROS and decreased mitochondrial content, we cotreated worms with XJB-5-131 (12.5–50 μM) and PFOS. We observed partial amelioration of DA neurodegeneration at 25 μM XJB-5-131 (91.87 ± 1.78, $p = .00013$) and 50 μM XJB-5-131 (90.62 ± 2.25, $p = .0023$) for total neurons in comparison to worms treated with 75 ppm PFOS alone (77.08 ± 0.90) (Figs. 6J and 6K). Further, we also measured the effect of XJB-5-131 on mitochondrial content, where we observed a significant alleviation in mitochondrial content in worms cotreated with 12.5 μM XJB-5-131 (1.37 ± 0.09, $p = .016$; $n = 3$) in comparison to worms treated with 75 ppm PFOS (Figure 6L).

Neuroprotective Effects of GSH

We also studied the effect of GSH on PFOS-mediated neurodegeneration. Worms were cotreated with GSH (0.125–2 mM) and 75 ppm PFOS. A single dose of GSH did not cause any alteration in PFOS-mediated neurodegeneration, whereas daily supplementation of GSH exhibited significant neuroprotection (Figure 7A). An increase in the percentage of intact neurons was observed at GSH levels of 0.125 mM (61.66 ± 3.99, $p = .0017$), 0.25 mM (68.75 ± 2.86, $p = .0003$), 0.5 mM (79.16 ± 5.59, $p = .0001$), 1 mM (72.45 ± 3.11, $p = .0001$), and 2 mM (65.62 ± 5.20, $p = .0006$) in comparison to 75 ppm PFOS alone (32.70 ± 3.85) (Figure 7B). Furthermore, considerable improvement in behavior corresponding to dopamine levels was also observed in worms subjected to cotreatment with 0.25 and 0.5 mM GSH as shown (Figure 7C). Significant differences in repulsion time were observed in worms cotreated with 0.25 mM GSH (2.11 ± 0.03, $p = .0001$) and 0.5 mM GSH (1.85 ± 0.07, $p = .0001$) in comparison to 5 ppm PFOS (3.09 ± 0.23) alone. At 25 ppm PFOS (3.40 ± 0.21), worms cotreated with 0.25 mM GSH (2.42 ± 0.09, $p = .0001$) and 0.5 mM GSH (1.90 ± 0.10, $p = .0001$) exhibited a significant decrease in repulsion time. Similarly, in worms treated with 50 ppm PFOS (4.38 ± 0.03), cotreatment with 0.25 mM GSH (3.07 ± 0.07, $p = .0001$) and 0.5 mM GSH (2.30 ± 0.10, $p = .0001$) exhibited a significant decrease in repulsion time. At the highest exposure level tested, 75 ppm PFOS (4.60 ± 0.21), considerable lowering in repulsion time was observed in worms cotreated with 0.25 mM GSH (3.04 ± 0.18, $p = .0001$) and 0.5 mM GSH (2.66 ± 0.17, $p = .0001$). These findings showed beneficial effects of GSH on dopamine levels in worms treated with PFOS. In order to further confirm out findings we eutilized BSO, which inhibits GSH biosynthesis through inhibition of gamma glutamylcysteine synthetase (Haddad, 2001). We observed a significant reduction in intact DA neurons upon cotreatment with BSO at 100 μM (60.83 ± 2.91, $p = .019$) and 200 μM (47.29 ± 4.18) in

comparison to 75 ppm PFOS alone (74.16 ± 1.36; $n = 3$) (Figure 7D). The exposure level of BSO utilized was not toxic to DA neurons (Figure 7E).

In light of the previous studies, where beneficial effects of NAC and HBA were observed on toxicant mediated mitochondrial affliction and DA cell loss (Sammi *et al.*, 2018), we cotreated the worms with NAC and HBA. In contrast to our previous studies, we observed a marginal decrease in percentage of intact neurons in worms cotreated with NAC (Supplementary Figs. S1A and S1B) and HBA (Supplementary Figs. S1C and S1D).

Neuroprotective Efficacy of BCD

β-Cyclodextrin has been reported to prevent or reverse the binding of PFOA to human serum albumin (Weiss-Errico *et al.*, 2018). We assessed the effects of BCD on PFOS-mediated neurodegeneration by cotreating worms with 75 ppm PFOS and BCD (150–300 μM) at 1, 1.5, and 2 times the equimolar concentration of PFOS. We observed significant neuroprotection at all BCD concentrations (Figure 8A). In terms of total neurons, increases in the percentage of intact neurons were observed in worms cotreated with BCD at concentrations of, 150 μM (96.66 ± 1.98, $p = .0001$), 225 μM (97.70 ± 1.45, $p = .0001$), and 300 μM (99.16 ± 0.41, $p = .0001$) in comparison to worms treated with 75 ppm PFOS alone (64.58 ± 3.89) (Figure 8B). Similar to the impact of BCD on PFOS-induced neurodegeneration, a significant protective effect on mitochondrial content, when exposed to 75 ppm PFOS was observed (Figure 8C) with BCD exposure levels of 150 μM (0.46 ± 0.04, $p = .0002$), 225 μM (0.30 ± 0.04, $p = .000$), and 300 μM (0.48 ± 0.03, $p = .0001$) in comparison to 75 ppm PFOS (0.03 ± 0.00) (Figure 8D).

To determine whether protection was simply due to decreased exposure, we also conducted time lag studies for different time points (BCD administered 12–72-h post-PFOS) in order to ascertain the time dependence amelioration of BCD. Here, we cotreated worms with 150 μM BCD and 75 ppm PFOS. We observed a significant increase in the percentage of intact neurons in comparison to 75 ppm PFOS. In terms of total neurons, compared with worms treated with 150 μM BCD for 72 h (93.75 ± 0.95), we only observed a significant difference in worms treated for 12 h (62.91 ± 3.50, $p = .0143$) and 24 h (81.66 ± 2.20, $p = .0001$) (Figure 8E). Notably, the percentage of intact neurons in worms cotreated with BCD for both 12 and 24 h ($p = .0002$ and .0001, respectively) treatment was significantly higher than 75 ppm PFOS alone.

We also tested whether BCD ameliorated dopamine-dependent behavioral deficits using the 1-nonanol assay. We observed a significant difference with respect to different exposure levels of PFOS (5–75 ppm) (Figure 8F). Modest, but significant decreases in repulsion time were observed in worms treated with 150 μM BCD at (1.68 ± 0.02, $p = .0309$) and 225 μM (1.57 ± 0.06, $p = .0035$) in comparison to untreated controls (2.01 ± 0.02). In worms treated with 5 ppm PFOS (2.53 ± 0.02), cotreatment with 150 μM BCD (1.46 ± 0.03, $p = .0001$) and 225 μM BCD (1.48 ± 0.07, $p = .0001$) led to a significant decrease in repulsion time. Similarly, worms cotreated with 150 μM BCD (1.67 ± 0.06, $p = .0001$) and 225 μM BCD (1.50 ± 0.01, $p = .0001$) also exhibited significant decreases in repulsion time in comparison to worms treated with 25 ppm PFOS (2.97 ± 0.07). In worms treated with 50 ppm PFOS (3.24 ± 0.10), worms cotreated with 150 μM BCD (1.67 ± 0.03, $p = .0001$) and 225 μM BCD (1.66 ± 0.05, $p = .0001$) exhibited a considerable reduction in repulsion time. At the highest exposure level studied, 75 ppm PFOS (4.05 ± 0.26), we observed a significant decrease in repulsion time in worms subjected to cotreatment with 150 μM BCD (1.76 ± 0.03, $p = .0001$) and 225 μM BCD (1.87 ± 0.11, $p = .0001$). These results implicated a positive effect of BCD on dopamine levels in worms challenged with PFOS.

Neurotoxicity of Additional and Alternative PFAS

We also tested other PFAS such as PFOA and GenX for their effect on DA neurons. PFOA, which differs with PFOS only in respect to the sulfonyl hydroxide group, did not show any signs of neurodegeneration within the tested exposure level range. Gen X, which is a replacement chemical for PFOS (Brandsma *et al.*, 2019), did show marginal neurodegeneration at the highest exposure levels (Table 2).

DISCUSSION

PFAS exposures represent a significant public health concern (Jian *et al.*, 2018; Sunderland *et al.*, 2019). Recently, we found dopamine levels to be selectively decreased in a sentinel species exposed to PFAS (Northern leopard frogs) (Foguth *et al.*, 2019). Additionally, PFAS produce neurotoxicity and behavioral deficits in *C. elegans* (Chen *et al.*, 2014). Thus, there is a clear indication that PFAS neurotoxicity may be important, but there are significant gaps in the literature with respect to which neuronal systems may be most sensitive. Here, nematode models were utilized to allow testing across a wide range of doses and to conduct mechanistic studies. Our data show that dopamine neurons are affected at lower exposure levels than those required to lesion other neuronal populations, suggesting heightened sensitivity. Functional assays showed that dopamine-dependent behavioral alterations correlated with the observed neuropathology, where acetylcholinergic-mediated function was unaffected. Thus, PFOS exposure should be examined for potential relevance to neurological diseases affecting DA neurons. In particular, relevance to Parkinson's disease should be evaluated given that selective DA neurodegeneration in animal models, including nematodes has repeatedly been utilized to identify risk factors and pathogenic mechanisms (Bornhorst *et al.*, 2014; Cannon and Greenamyre, 2010). Indeed, our mechanistic studies implicated pathogenic features important to Parkinson's disease, including oxidative damage and mitochondrial impairment. Finally, we identified specific neuroprotective strategies. Overall, the observed selective DA pathology suggests that the risk of chronic PFAS exposure, even at low exposure levels, should be evaluated for long-term neurological consequences.

Exposure levels were chosen based on environmental and biological PFAS levels and those used for established DA neurotoxicants in nematodes (Table 1). Here, it is worth noting that PFOS in human blood has been detected within the tested range (≥25 ppm for most assays) (Olsen *et al.*, 2003). Moreover, effects on mitochondrial endpoints were evident at exposures as low as 1 ppm. PFOS is known to bioconcentrate in aquatic animals (Arnot and Gobas, 2006; Higgins *et al.*, 2007; Jeon *et al.*, 2010). Similarly, we observed up to a 13-fold bioconcentration in *C. elegans*. PFAS accumulate in mammalian brain, suggesting that it will be critical to study total brain and subregional half-lives (blood is usually reported) and adjust dosing regimens accordingly (Dassuncao *et al.*, 2019; Eggers Pedersen *et al.*, 2015).

Reactive oxygen species generation is a critical aspect of Parkinson's disease pathogenesis (Dias *et al.*, 2013). Thus, we examined ROS in PFOS-treated worms. A decrease in superoxide ions was observed at lower exposure levels. This finding is consistent with previous reports, where increased superoxide dismutase activity has been reported as response to PFOS

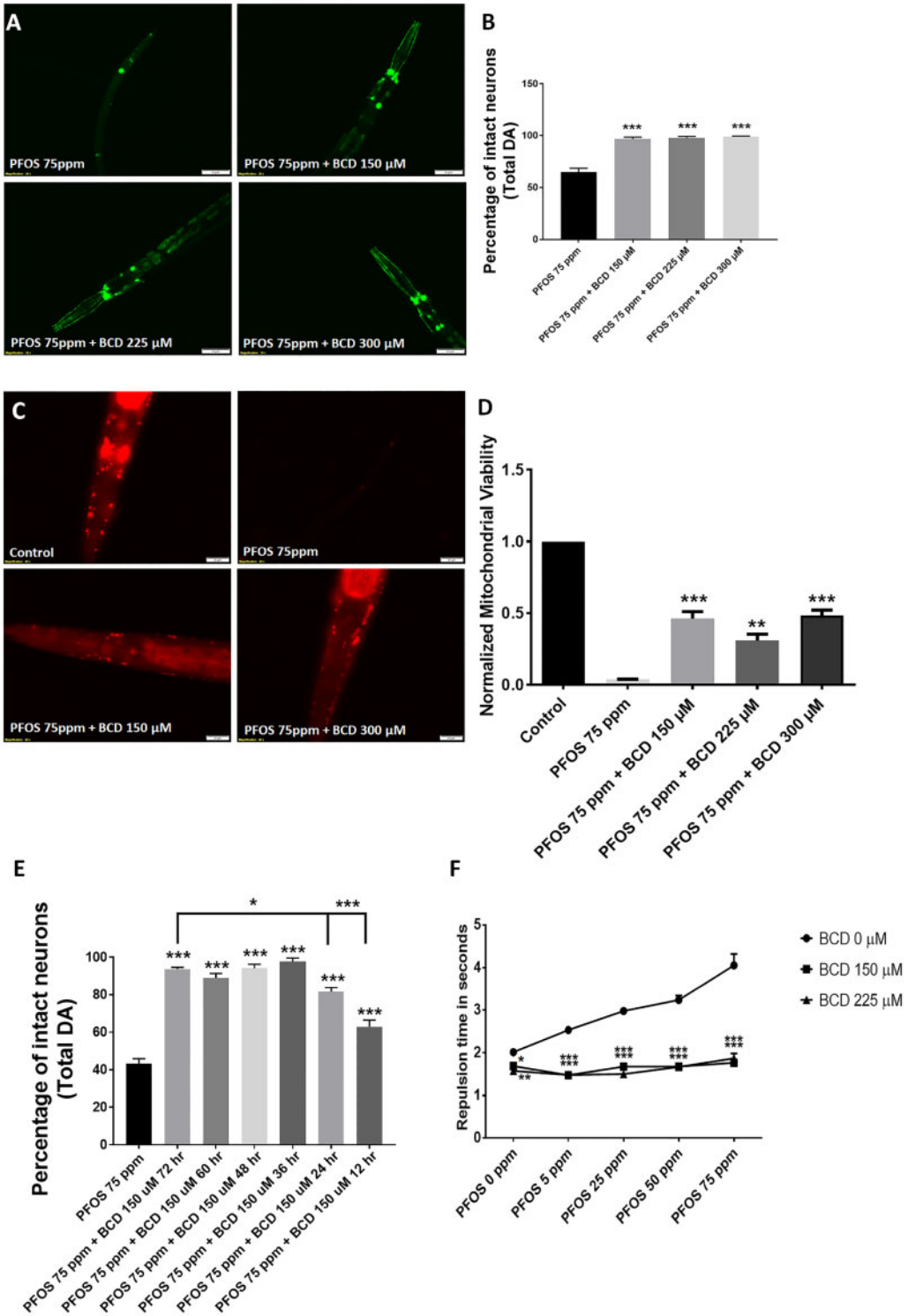

Figure 8. β-Cyclodextrin (BCD) ameliorates PFOS-mediated neurodegeneration. Treatment with BCD (150, 225, and 300 µM) prevented PFOS (75 ppm) mediated neurodegeneration (A, B). Further, BCD treatment prevented reductions in mitochondrial content (C, D). The effects of delayed BCD (post-PFOS administration) were determined with a 12–72-h lag treatment for 2 exposure levels, 150 and 200 µM. In worms cotreated with 150 µM BCD, reduced neuroprotective efficacy was not observed until treatment was delayed for 48–72 h (E). Worms treated with BCD exhibited functional improvement in dopamine-dependent 1-nonanol repulsion in comparison to untreated worms across different exposure level of PFOS (F). Treatments conducted for a duration of 72 h. Data are presented as mean ± S.E.M. Data were analyzed by one-way ANOVA (C, D, E) or by two-way ANOVA (F) for grouped analysis and followed by Dunnett's post hoc test. $^{*}p < .05$, $^{**}p < .01$, and $^{***}p < .001$ ($n = 3$). Scale bar represents 50 µm (A) and 20 µm (C).

Table 2. PFAS Tested for Selective DA Neurotoxicity

PFAS	Exposure Level Range Tested for Neurodegeneration (ppm)	Threshold for DA Neurodegeneration	Threshold for Non-DA Neurodegeneration	Selective Neurodegeneration (Yes/No)
PFOA	25–200	Not found	Not tested	Not detected at tested exposure levels
PFOS	25–200	25	100	Yes
GenX	25–200	200	Not tested	Yes

Numerous PFAS were evaluated for evidence of neurodegeneration. Selective DA neurodegeneration was identified where the threshold (lowest does) to induce statistically significant DA neurodegeneration was lower than that to induce non-DA neurodegeneration (significant effects on GABA, 5-HT, or ACh neurons)—lowest exposure level to affect one of these populations is reported. ND = not detectable.

administration in multiple models (Chen *et al.*, 2014; Hu and Hu, 2009; Liu *et al.*, 2007). A further increase in PFOS exposure levels, led to an eventual elevation in superoxide levels. In contrast, total ROS levels exhibited a concentration-dependent increase with respect to PFOS, suggesting contribution from sources other than superoxide or a biochemical response to PFOS-induced superoxide alterations. To further explore a potential contribution of superoxide, we first cotreated worms with low exposure levels of the superoxide generator, juglone (Ishii *et al.*, 1990; Tawe *et al.*, 1998; Vanfleteren, 1993), and then studied the effect of DA neurons in mutants for mitochondrial SOD (*sod-3*, [gk235] with 390-bp deletion expected to produce a loss-of-function). Here, we did not observe any alteration in the percentage of intact neurons in worms treated with juglone, suggesting a limited role of superoxide ions in PFOS-mediated neurodegeneration. This implied that the increased SOD activity might be a protective response toward oxidative stress. Notably, exposure levels of juglone demonstrated increase in superoxide levels and total ROS. Exposure level rationale was concluded relying on fact that higher exposure levels (approximately 20 μM) produced DA cell loss. In order to further corroborate our findings, we utilized mutants for mitochondrial SOD (*sod-3*). The rationale for using mitochondrial SOD mutants was that in our studies, mitochondria were found to be a likely key pathogenic target. Further, utilizing mutants for cellular SOD would evoke a larger, generalized SOD deficiency, which may serve as a confounding factor. Here, we utilized the mutation that does not generate a near complete SOD deficiency. We found that mitochondrial SOD mutants were both more vulnerable to PFOS-mediated neurodegeneration and also exhibited a developmental delay. Normal worms exhibited decreases in the percentage of intact neurons in an exposure level-dependent manner; however, in SOD-3 mutants, a slight decrease in PFOS associated neuropathology was observed at 100 ppm in comparison to 75 ppm, implying that larval stages alter the response to PFOS-mediated neurodegeneration.

Mitochondrial dysfunction is a critical feature of Parkinson's disease pathogenesis (Reddy, 2009; Schon and Manfredi, 2003; Young, 2009). We observed a significant concentration-dependent decrease in mitochondrial content at levels as low as 1 ppm. It is noteworthy that a 1-ppm exposure is comparable to the range of PFOS levels found in blood samples from American donors (0.0041–1.656 ppm) (Olsen *et al.*, 2003). Similar to the findings in worms, we also observed significant elevation in ROS levels in galactose-supplemented SH-SY5Y cells treated with PFOS. Further, we observed a significant decrease in proton leak and nonmitochondrial oxygen consumption, with no changes in other mitochondrial functions. Depletion of both oxygen consumption rate implied the stressed condition of mitochondria, supporting our findings from the MitoTracker studies conducted in worms. It is possible that PFOS-induced decreases in oxygen consumption rate stemmed from decreased mitochondrial content. However, this correlation could not be established in the studies here because bioenergetic studies were conducted in SH-SY5Y cells and mitochondrial content was measured in nematodes. Depletion of both oxygen consumption rate and extracellular acidification rate suggests the possibility of a general, regulated decrease in energetics. Here, future studies in both highly glycolic (glucose supplemented) cells and those more reliant on oxidative phosphorylation (galactose supplemented) may be useful (de Rus Jacquet *et al.*, 2017; Marroquin *et al.*, 2007).

We also tested whether antioxidants and mitochondrial activators previously shown to rescue *C. elegans* exposed to toxicants causing DA neuronal loss would be protective (Sammi *et al.*, 2018). Surprisingly, we did not observe detectable neuroprotection; rather, a marginal decrease in the percentage of intact neurons in worms (data shown in supplementary material; studies with HBA and NAC). A potential explanation for the lack of efficacy of HBA and NAC relative to the positive findings in other nematode PD models could be due to the inability of the involved pathways in circumventing PFOS-mediated neurodegeneration. N-acetyl-L-cysteine is a generalized activator of mitochondrial complexes I, IV, and V (Cocco *et al.*, 2005; Kamboj and Sandhir, 2011; Miquel *et al.*, 1995; Soiferman *et al.*, 2014), besides also being involved in GSH maintenance/metabolism (Atkuri *et al.*, 2007; Kerksick and Willoughby, 2005). We hypothesized that PFOS could directly affect the GSH biosynthetic pathway; a mechanism that would limit the efficacy of NAC. We also observed similar results upon inhibition of GSH biosynthesis in later studies using BSO. Furthermore, a possible explanation of lack of HBA mediated neuroprotection could be due to effects on complex II which is involved in HBA mediated enhancement of oxidative phosphorylation (Tieu *et al.*, 2003). Indeed, alterations in GSH biosynthesis are postulated to be a primary pathogenic pathway in Parkinson's disease (Martin and Teismann, 2009). We also tested a targeted mitochondrial ROS scavenger, XJB-5-131, that contains the electron and radical scavenger 4-AT, which also functions as an SOD mimetic (Khattab 2006), and a mitochondrial membrane targeting sequences derived from the antibiotic gramicidin S. Our initial studies on worms challenged with millimolar MPP^+ exhibited significant amelioration in response to micromolar XJB-5-131. Further, we cotreated worms with PFOS and XJB-5-131 but only observed a marginal ameliorative effect of XJB-5-131 against PFOS. This marginal effect could be attributed to the fact that 4-AT like Tempo is an SOD mimetic and an effective superoxide radical ion scavenger (Aksu *et al.*, 2015; Khattab, 2006), but DA neuronal loss might be attributed largely to other ROS besides superoxide ions.

Furthermore, hydrogen peroxide levels are not substantially influenced by XJB-5-131 (Wenz *et al.*, 2018). Surprisingly, XJB-5-131 when tested for its effect on mitochondrial content, exhibited only partial rescue against PFOS-treated worms.

We also tested the effect of GSH on PFOS afflicted DA neuronal loss. Worms treated once with GSH did not exhibit significantly increased survival, which might be because GSH is oxidized in solution (Kalebic *et al.*, 1991). However, daily treatment with GSH exhibited a significant amount of neuroprotection in a concentration-dependent manner. Furthermore, we also observed a significant rescue of dopamine-related behavior in worms treated with 0.25 and 0.5 mM GSH. Furthermore, BSO, an inhibitor of GSH biosynthesis (Haddad, 2001) also exhibited enhanced neurotoxicity when cotreated with PFOS. Of note, the delay in neuroprotective effects of GSH supplementation may have been because mitochondria lack inherent machinery to synthesize GSH and rely solely on cytosolic GSH to maintain intramitochondrial GSH pool, which has to be moved inside mitochondria against the electrophoretic gradient in an ATP driven manner (Fernandez-Checa *et al.*, 1997).

Taken together, these findings suggest that mitochondria are a key pathogenic target and mechanistic and neuroprotective studies suggest specific biochemical mechanisms.

Few therapeutic options currently have been tested for PFAS. β-Cyclodextrin is a cyclic carbohydrate based chelator of hydrophobic substances that has been demonstrated to encapsulate PFOA, with 2 BCD molecules required to encapsulate 1 eight-carbon PFAS (Weiss-Errico and O'Shea, 2017). Of significance to *in vivo* systems, BCD has been reported to reduce binding of PFOA to human serum albumin (Weiss-Errico *et al.*, 2018). In general, these citations suggest a 1:1 molarity or greater, in accordance to the properties of the amphiphilic chelator BCD. To date, there is limited knowledge on whether BCD may protect from a sulfonated PFAS. Thus, we tested BCD at 1×, 1.5×, and 2× the stoichiometry of PFOS. We observed significant neuroprotection in worms from PFOS at all tested exposure levels. Cotreatment bears limited clinical relevance and protection could be simply due to preventing PFAS from entering the tissue. Thus, we determined the effect delayed BCD administration. Given that BCD was protective when administered 12 and 24 h after PFOS (only at 72 h did the effect diminish), these results suggest a promising chelation based neuroprotective effect of BCD against PFOS-induced neurotoxicity. Additionally, the time lag studies highlighted that BCD confers neuroprotection upon both immediate and delayed administration.

Nematode models have many advantages in assessing neurotoxicity. However, it is clear that these results should prompt studies in higher order systems and epidemiological studies in humans. Of further note, DA neuron degeneration in nematodes is often linked to potential relevance to Parkinson's disease, though relevance to other DA systems in higher order species, including the reward pathway and neuroendocrine function will also need to be evaluated.

In summary, multiple neuropathology and biochemical endpoints suggest that DA neurons are especially sensitive to PFOS exposure, and that potential therapeutic leads include amphiphilic chelators such as BCD, antioxidants such as GSH, and targeted SOD mimetics such as XJB-5-131. Given the public health concern of PFOS and other PFAS, along with neurotoxicity findings here and in a recent neurochemical study, the role of PFAS in adverse neurological outcomes in humans should receive significant attention (Foguth *et al.*, 2019).

SUPPLEMENTARY DATA

Supplementary data are available at *Toxicological Sciences* online.

DECLARATION OF CONFLICTING INTERESTS

The authors declare the following potential conflicts. Peter Wipf: coinventor on patents filed for XJB-5-131 and held by the University of Pittsburgh. Linda Lee: expert reviewer for the California Environmental Protection Agency (Cal/EPA) for the "Proposed Adoption of Carpet and Rugs Containing Perfluoroalkyl or Polyfluoroalkyl Substances as a Priority Product." Called on by lawyers as an expert witness on the occurrence, fate, and potential harm associate with PFAS. The other authors declare they have no actual or potential competing financial interests. The authors who certify that all actual or potential competing financial interests have been declared and that the authors' freedom to design, conduct, interpret, and publish research is not compromised by any controlling sponsor as a condition of review and publication.

FUNDING

This work was supported by the National Institute of Environmental Health Sciences at the National Institutes (R01ES025750 to J.R.C.) and the Ralph W. and Grace M. Showalter Research Trust (to J.R.C.). The authors would also like to acknowledge *C. elegans* Gene Knockout Consortium. Strains were provided by the Caenorhabditis Genetics Center, which is funded by National Institute of Health Office of Research Infrastructure Programs (P40 OD010440).

REFERENCES

Aksu, U., Ergin, B., Bezemer, R., Kandil, A., Milstein, D. M., Demirci-Tansel, C., and Ince, C. (2015). Scavenging reactive oxygen species using tempol in the acute phase of renal ischemia/reperfusion and its effects on kidney oxygenation and nitric oxide levels. *Intensive Care Med. Exp.* **3**, 57.

Alexander, A. G., Marfil, V., and Li, C. (2014). Use of *Caenorhabditis elegans* as a model to study Alzheimer's disease and other neurodegenerative diseases. *Front. Genet.* **5**, 279.

Arnot, J. A., and Gobas, F. A. P. C. (2006). A review of bioconcentration factor (BCF) and bioaccumulation factor (BAF) assessments for organic chemicals in aquatic organisms. *Environ. Rev.* **14**, 257–297.

Atkuri, K. R., Mantovani, J. J., Herzenberg, L. A., and Herzenberg, L. A. (2007). N-acetylcysteine—A safe antidote for cysteine/glutathione deficiency. *Curr. Opin. Pharmacol.* **7**, 355–359.

Baidya, M., Genovez, M., Torres, M., and Chao, M. Y. (2014). Dopamine modulation of avoidance behavior in *Caenorhabditis elegans* requires the NMDA receptor NMR-1. *PLoS One* **9**, e102958.

Banner, W., Jr, Koch, M., Capin, D. M., Hopf, S. B., Chang, S., and Tong, T. G. (1986). Experimental chelation therapy in chromium, lead, and boron intoxication with N-acetylcysteine and other compounds. *Toxicol. Appl. Pharmacol.* **83**, 142–147.

Bargmann, C. I., Hartwieg, E., and Horvitz, H. R. (1993). Odorant-selective genes and neurons mediate olfaction in *C. elegans*. *Cell* **74**, 515–527.

Benedetto, A., Au, C., Avila, D. S., Milatovic, D., and Aschner, M. (2010). Extracellular dopamine potentiates Mn-induced oxidative stress, lifespan reduction, and dopaminergic

neurodegeneration in a BLI-3-dependent manner in *Caenorhabditis elegans*. *PLoS Genet* **6**, e1001084.

Bornhorst, J., Chakraborty, S., Meyer, S., Lohren, H., Brinkhaus, S. G., Knight, A. L., Caldwell, K. A., Caldwell, G. A., Karst, U., Schwerdtle, T., *et al*. (2014). The effects of pdr1, djr1.1 and pink1 loss in manganese-induced toxicity and the role of alpha-synuclein in *C. elegans*. *Metallomics* **6**, 476–490.

Brandsma, S. H., Koekkoek, J. C., van Velzen, M. J. M., and de Boer, J. (2019). The PFOA substitute GenX detected in the environment near a fluoropolymer manufacturing plant in the Netherlands. *Chemosphere* **220**, 493–500.

Cannon, J. R., and Greenamyre, J. T. (2010). Neurotoxic in vivo models of Parkinson's disease recent advances. *Prog. Brain Res.* **184**, 17–33.

Chen, N., Li, J., Li, D., Yang, Y., and He, D. (2014). Chronic exposure to perfluorooctane sulfonate induces behavior defects and neurotoxicity through oxidative damages, in vivo and in vitro. *PLoS One* **9**, e113453.

Chengelis, C. P., Kirkpatrick, J. B., Myers, N. R., Shinohara, M., Stetson, P. L., and Sved, D. W. (2009). Comparison of the toxicokinetic behavior of perfluorohexanoic acid (PFHxA) and nonafluorobutane-1-sulfonic acid (PFBS) in cynomolgus monkeys and rats. *Reprod. Toxicol.* **27**, 400–406.

Chernivec, E., Cooper, J., and Naylor, K. (2018). Exploring the effect of rotenone—A known inducer of Parkinson's disease-on mitochondrial dynamics in *Dictyostelium discoideum*. *Cells* **7**, 201.

Chikka, M. R., Anbalagan, C., Dvorak, K., Dombeck, K., and Prahlad, V. (2016). The mitochondria-regulated immune pathway activated in the *C. elegans* intestine is neuroprotective. *Cell Rep.* **16**, 2399–2414.

Cocco, T., Sgobbo, P., Clemente, M., Lopriore, B., Grattagliano, I., Di Paola, M., and Villani, G. (2005). Tissue-specific changes of mitochondrial functions in aged rats: Effect of a long-term dietary treatment with N-acetylcysteine. *Free Radic. Biol. Med.* **38**, 796–805.

Dassuncao, C., Pickard, H., Pfohl, M., Tokranov, A. K., Li, M., Mikkelsen, B., Slitt, A., and Sunderland, E. M. (2019). Phospholipid levels predict the tissue distribution of poly- and perfluoroalkyl substances in a marine mammal. *Environ. Sci. Technol. Lett.* **6**, 119–125.

de Rus Jacquet, A., Timmers, M., Ma, S. Y., Thieme, A., McCabe, G. P., Vest, J. H. C., Lila, M. A., and Rochet, J. C. (2017). Lumbee traditional medicine: Neuroprotective activities of medicinal plants used to treat Parkinson's disease-related symptoms. *J. Ethnopharmacol.* **206**, 408–425.

Dias, V., Junn, E., and Mouradian, M. M. (2013). The role of oxidative stress in Parkinson's disease. *J. Parkinsons Dis.* **3**, 461–491.

Eggers Pedersen, K., Basu, N., Letcher, R., Greaves, A. K., Sonne, C., Dietz, R., and Styrishave, B. (2015). Brain region-specific perfluoroalkylated sulfonate (PFSA) and carboxylic acid (PFCA) accumulation and neurochemical biomarker responses in east Greenland polar bears (*Ursus maritimus*). *Environ. Res.* **138**, 22–31.

epa.gov. *Basic Information on PFAS*. https://www.epa.gov/pfas/basic-information-pfas

Fernandez-Checa, J. C., Kaplowitz, N., Garcia-Ruiz, C., Colell, A., Miranda, M., Mari, M., Ardite, E., and Morales, A. (1997). GSH transport in mitochondria: Defense against TNF-induced oxidative stress and alcohol-induced defect. *Am. J. Physiol.* **273**, G7–G17.

Foguth, R. M., Flynn, R. W., de Perre, C., Iacchetta, M., Lee, L. S., Sepulveda, M. S., and Cannon, J. R. (2019). Developmental exposure to perfluorooctane sulfonate (PFOS) and perfluorooctanoic acid (PFOA) selectively decreases brain dopamine levels in Northern leopard frogs. *Toxicol. Appl. Pharmacol.* **377**, 114623.

Gaffney, C. J., Bass, J. J., Barratt, T. F., and Szewczyk, N. J. (2014). Methods to assess subcellular compartments of muscle in *C. elegans*. *J. Vis. Exp.* **93**, e52043.

Gonzalez-Hunt, C. P., Leung, M. C., Bodhicharla, R. K., McKeever, M. G., Arrant, A. E., Margillo, K. M., Ryde, I. T., Cyr, D. D., Kosmaczewski, S. G., Hammarlund, M., *et al*. (2014). Exposure to mitochondrial genotoxins and dopaminergic neurodegeneration in *Caenorhabditis elegans*. *PLoS One* **9**, e114459.

Greenamyre, J. T., Betarbet, R., and Sherer, T. B. (2003). The rotenone model of Parkinson's disease: Genes, environment and mitochondria. *Parkinsonism Relat. Disord.* **9(Suppl. 2)**, S59–S64.

Haddad, J. J. (2001). L-Buthionine-(S,R)-sulfoximine, an irreversible inhibitor of gamma-glutamylcysteine synthetase, augments LPS-mediated pro-inflammatory cytokine biosynthesis: Evidence for the implication of an IkappaB-alpha/NF-kappaB insensitive pathway. *Eur. Cytokine Netw.* **12**, 614–624.

Higgins, C. P., McLeod, P. B., MacManus-Spencer, L. A., and Luthy, R. G. (2007). Bioaccumulation of perfluorochemicals in sediments by the aquatic oligochaete *Lumbriculus variegatus*. *Environ. Sci. Technol.* **41**, 4600–4606.

Hoff, P. T., Scheirs, J., Van de Vijver, K., Van Dongen, W., Esmans, E. L., Blust, R., and De Coen, W. (2004). Biochemical effect evaluation of perfluorooctane sulfonic acid-contaminated wood mice (*Apodemus sylvaticus*). *Environ. Health Perspect.* **112**, 681–686.

Hoover, G. M., Chislock, M. F., Tornabene, B. J., Guffey, S. C., Choi, Y. J., De Perre, C., Hoverman, J. T., Lee, L. S., and Sepúlveda, M. S. (2017). Uptake and depuration of four per/polyfluoroalkyl substances (PFASS) in northern leopard frog *Rana pipiens* tadpoles. *Environ. Sci. Technol. Lett.* **4**, 399–403.

Hu, X. Z., and Hu, D. C. (2009). Effects of perfluorooctanoate and perfluorooctane sulfonate exposure on hepatoma Hep G2 cells. *Arch. Toxicol.* **83**, 851–861.

Hunt, P. R. (2017). The *C. elegans* model in toxicity testing. *J. Appl. Toxicol.* **37**, 50–59.

Ishii, N., Takahashi, K., Tomita, S., Keino, T., Honda, S., Yoshino, K., and Suzuki, K. (1990). A methyl viologen-sensitive mutant of the nematode *Caenorhabditis elegans*. *Mutat. Res.* **237**, 165–171.

Jeon, J., Kannan, K., Lim, H. K., Moon, H. B., and Kim, S. D. (2010). Bioconcentration of perfluorinated compounds in blackrock fish, *Sebastes schlegeli*, at different salinity levels. *Environ. Toxicol. Chem.* **29**, 2529–2535.

Ji, J., Kline, A. E., Amoscato, A., Samhan-Arias, A. K., Sparvero, L. J., Tyurin, V. A., Tyurina, Y. Y., Fink, B., Manole, M. D., and Puccio, A. M. (2012). Lipidomics identifies cardiolipin oxidation as a mitochondrial target for redox therapy of brain injury. *Nat. Neurosci.* **15**, 1407–1413.

Jian, J. M., Chen, D., Han, F. J., Guo, Y., Zeng, L., Lu, X., and Wang, F. (2018). A short review on human exposure to and tissue distribution of per- and polyfluoroalkyl substances (PFASs). *Sci. Total Environ.* **636**, 1058–1069.

Johansson, N., Eriksson, P., and Viberg, H. (2009). Neonatal exposure to PFOS and PFOA in mice results in changes in proteins which are important for neuronal growth and synaptogenesis in the developing brain. *Toxicol. Sci.* **108**, 412–418.

Jonassen, T., Larsen, P. L., and Clarke, C. F. (2001). A dietary source of coenzyme Q is essential for growth of long-lived

Caenorhabditis elegans clk-1 mutants. *Proc. Natl. Acad. Sci. U.S.A.* **98**, 421–426.

Kalebic, T., Kinter, A., Poli, G., Anderson, M. E., Meister, A., and Fauci, A. S. (1991). Suppression of human immunodeficiency virus expression in chronically infected monocytic cells by glutathione, glutathione ester, and N-acetylcysteine. *Proc. Natl. Acad. Sci. U.S.A.* **88**, 986–990.

Kalyanaraman, B., Darley-Usmar, V., Davies, K. J., Dennery, P. A., Forman, H. J., Grisham, M. B., Mann, G. E., Moore, K., Roberts, L. J., 2nd, and Ischiropoulos, H. (2012). Measuring reactive oxygen and nitrogen species with fluorescent probes: Challenges and limitations. *Free Radic. Biol. Med.* **52**, 1–6.

Kamboj, S. S., and Sandhir, R. (2011). Protective effect of N-acetylcysteine supplementation on mitochondrial oxidative stress and mitochondrial enzymes in cerebral cortex of streptozotocin-treated diabetic rats. *Mitochondrion* **11**, 214–222.

Kaur, S., Sammi, S. R., Jadiya, P., and Nazir, A. (2012). RNAi of cat-2, a putative tyrosine hydroxylase, increases alpha synuclein aggregation and associated effects in transgenic *C. elegans*. *CNS Neurol. Disord. Drug Targets* **11**, 387–394.

Kerksick, C., and Willoughby, D. (2005). The antioxidant role of glutathione and N-acetyl-cysteine supplements and exercise-induced oxidative stress. *J. Int. Soc. Sports Nutr.* **2**, 38–44.

Khattab, M. M. (2006). TEMPOL, a membrane-permeable radical scavenger, attenuates peroxynitrite- and superoxide anion-enhanced carrageenan-induced paw edema and hyperalgesia: A key role for superoxide anion. *Eur. J. Pharmacol.* **548**, 167–173.

Krainz, T., Gaschler, M. M., Lim, C., Sacher, J. R., Stockwell, B. R., and Wipf, P. (2016). A mitochondrial-targeted nitroxide is a potent inhibitor of ferroptosis. *ACS Cent. Sci.* **2**, 653–659.

Larsen, P. B., and Giovalle, E. (2015). *Perfluoroalkylated Substances: PFOA, PFOS and PFOSA*. Environmental Project No. 1665. The Danish Environmental Protection Agency, Copenhagen, Denmark.

Lee, I., and Viberg, H. (2013). A single neonatal exposure to perfluorohexane sulfonate (PFHxS) affects the levels of important neuroproteins in the developing mouse brain. *Neurotoxicology* **37**, 190–196.

Li, W., He, Q. Z., Wu, C. Q., Pan, X. Y., Wang, J., Tan, Y., Shan, X. Y., and Zeng, H. C. (2015). PFOS disturbs BDNF-ERK-CREB signalling in association with increased MicroRNA-22 in SH-SY5Y cells. *BioMed Res. Int.* **2015**, Article ID 302653.

Liu, C., Yu, K., Shi, X., Wang, J., Lam, P. K., Wu, R. S., and Zhou, B. (2007). Induction of oxidative stress and apoptosis by PFOS and PFOA in primary cultured hepatocytes of freshwater tilapia (*Oreochromis niloticus*). *Aquat. Toxicol.* **82**, 135–143.

Lucio, D., Martinez-Oharriz, M. C., Gonzalez-Navarro, C. J., Navarro-Herrera, D., Gonzalez-Gaitano, G., Radulescu, A., and Irache, J. M. (2018). Coencapsulation of cyclodextrins into poly(anhydride) nanoparticles to improve the oral administration of glibenclamide. A screening on *C. elegans*. *Colloids Surf. B Biointerfaces* **163**, 64–72.

Ma, L., Zhao, Y., Chen, Y., Cheng, B., Peng, A., and Huang, K. (2018). *Caenorhabditis elegans* as a model system for target identification and drug screening against neurodegenerative diseases. *Eur. J. Pharmacol.* **819**, 169–180.

Mahoney, T. R., Luo, S., and Nonet, M. L. (2006). Analysis of synaptic transmission in *Caenorhabditis elegans* using an Aldicarb-sensitivity assay. *Nat. Protoc.* **1**, 1772–1777.

Marroquin, L. D., Hynes, J., Dykens, J. A., Jamieson, J. D., and Will, Y. (2007). Circumventing the Crabtree effect: Replacing media glucose with galactose increases susceptibility of HepG2 cells to mitochondrial toxicants. *Toxicol. Sci.* **97**, 539–547.

Martin, H. L., and Teismann, P. (2009). Glutathione—A review on its role and significance in Parkinson's disease. *FASEB J.* **23**, 3263–3272.

Martinez, B. A., Kim, H., Ray, A., Caldwell, G. A., and Caldwell, K. A. (2015). A bacterial metabolite induces glutathione-tractable proteostatic damage, proteasomal disturbances, and PINK1-dependent autophagy in *C. elegans*. *Cell Death Dis.* **6**, e1908.

Miquel, J., Ferrandiz, M. L., De Juan, E., Sevila, I., and Martinez, M. (1995). N-acetylcysteine protects against age-related decline of oxidative phosphorylation in liver mitochondria. *Eur. J. Pharmacol.* **292**, 333–335.

Mulcahy, B., Holden-Dye, L., and O'Connor, V. (2013). Pharmacological assays reveal age-related changes in synaptic transmission at the *Caenorhabditis elegans* neuromuscular junction that are modified by reduced insulin signalling. *J. Exp. Biol.* **216**(Pt 3), 492–501.

Nass, R., Hall, D. H., Miller, D. M., 3rd, and Blakely, R. D. (2002). Neurotoxin-induced degeneration of dopamine neurons in *Caenorhabditis elegans*. *Proc. Natl. Acad. Sci. U.S.A.* **99**, 3264–3269.

Oh, S. I., Park, J. K., and Park, S. K. (2015). Lifespan extension and increased resistance to environmental stressors by N-acetyl-L-cysteine in *Caenorhabditis elegans*. *Clinics (Sao Paulo)* **70**, 380–386.

O'Hagan, D. (2008). Understanding organofluorine chemistry. An introduction to the C-F bond. *Chem. Soc. Rev.* **37**, 308–319.

Olsen, G. W., Church, T. R., Miller, J. P., Burris, J. M., Hansen, K. J., Lundberg, J. K., Armitage, J. B., Herron, R. M., Medhdizadehkashi, Z., Nobiletti, J. B., *et al.* (2003). Perfluorooctanesulfonate and other fluorochemicals in the serum of American Red Cross adult blood donors. *Environ. Health Perspect.* **111**, 1892–1901.

Onishchenko, N., Fischer, C., Wan Ibrahim, W. N., Negri, S., Spulber, S., Cottica, D., and Ceccatelli, S. (2011). Prenatal exposure to PFOS or PFOA alters motor function in mice in a sex-related manner. *Neurotox. Res.* **19**, 452–461.

Park, J. S., Davis, R. L., and Sue, C. M. (2018). Mitochondrial Dysfunction in Parkinson's Disease: New Mechanistic Insights and Therapeutic Perspectives. *Curr Neurol Neurosci Rep* **18**, 21.

Polyzos, A., Holt, A., Brown, C., Cosme, C., Wipf, P., Gomez-Marin, A., Castro, M. R., Ayala-Pena, S., and McMurray, C. T. (2016). Mitochondrial targeting of XJB-5-131 attenuates or improves pathophysiology in HdhQ150 animals with well-developed disease phenotypes. *Hum. Mol. Genet.* **25**, 1792–1802.

Post, G. B., Cohn, P. D., and Cooper, K. R. (2012). Perfluorooctanoic acid (PFOA), an emerging drinking water contaminant: A critical review of recent literature. *Environ. Res.* **116**, 93–117.

Pu, P., and Le, W. (2008). Dopamine neuron degeneration induced by MPP+ is independent of CED-4 pathway in *Caenorhabditis elegans*. *Cell Res.* **18**, 978–981.

Ray, A., Martinez, B. A., Berkowitz, L. A., Caldwell, G. A., and Caldwell, K. A. (2014). Mitochondrial dysfunction, oxidative stress, and neurodegeneration elicited by a bacterial metabolite in a *C. elegans* Parkinson's model. *Cell Death Dis.* **5**, e984.

Reddy, P. H. (2009). Role of mitochondria in neurodegenerative diseases: Mitochondria as a therapeutic target in Alzheimer's disease. *CNS Spectr.* **14(8 Suppl. 7)**, 8–13. discussion 16-8.

Sammi, S. R., Agim, Z. S., and Cannon, J. R. (2018). From the cover: Harmane-induced selective dopaminergic neurotoxicity in *Caenorhabditis elegans*. *Toxicol. Sci.* **161**, 335–348.

Sammi, S. R., Trivedi, S., Rath, S. K., Nagar, A., Tandon, S., Kalra, A., and Pandey, R. (2017). 1-Methyl-4-propan-2-ylbenzene from *Thymus vulgaris* attenuates cholinergic dysfunction. *Mol. Neurobiol.* **54**, 5468–5481.

Sanchez Garcia, D., Sjodin, M., Hellstrandh, M., Norinder, U., Nikiforova, V., Lindberg, J., Wincent, E., Bergman, A., Cotgreave, I., and Munic Kos, V. (2018). Cellular accumulation and lipid binding of perfluorinated alkylated substances (PFASs)—A comparison with lysosomotropic drugs. *Chem. Biol. Interact.* **281**, 1–10.

Sanyal, S., Wintle, R. F., Kindt, K. S., Nuttley, W. M., Arvan, R., Fitzmaurice, P., Bigras, E., Merz, D. C., Hebert, T. E., van der Kooy, D., *et al.* (2004). Dopamine modulates the plasticity of mechanosensory responses in *Caenorhabditis elegans*. *EMBO J* **23**, 473–482.

Schneider, C. A., Rasband, W. S., and Eliceiri, K. W. (2012). NIH Image to ImageJ: 25 years of image analysis. *Nat Methods.* **9**, 671–675.

Schon, E. A., and Manfredi, G. (2003). Neuronal degeneration and mitochondrial dysfunction. *J. Clin. Invest.* **111**, 303–312.

Senchuk, M. M., Dues, D. J., and Van Raamsdonk, J. M. (2017). Measuring oxidative stress in *Caenorhabditis elegans*: Paraquat and Juglone sensitivity assays. *Bio-Protocol* **7**, e2086.

Smita, S. S., Raj Sammi, S., Laxman, T. S., Bhatta, R. S., and Pandey, R. (2017). Shatavarin IV elicits lifespan extension and alleviates Parkinsonism in *Caenorhabditis elegans*. *Free Radic. Res.* **51**, 954–969.

Soiferman, D., Ayalon, O., Weissman, S., and Saada, A. (2014). The effect of small molecules on nuclear-encoded translation diseases. *Biochimie* **100**, 184–191.

Slotkin, T. A., MacKillop, E. A., Melnick, R. L., Thayer, K. A., and Seidler, F. J. (2008). Developmental neurotoxicity of perfluorinated chemicals modeled in vitro. *Environmental health perspectives* **116**, 716–722.

Steenland, K., Fletcher, T., and Savitz, D. A. (2010). Epidemiologic evidence on the health effects of perfluorooctanoic acid (PFOA). *Environ. Health Perspect.* **118**, 1100–1108.

Stiernagle, T. (2006). Maintenance of *C. elegans*. In *WormBook* (D. Fay, Ed.), The C. elegans Research Community. WormBook, doi/10.1895/wormbook.1.101.1, http://www.wormbook.org.

Sunderland, E. M., Hu, X. C., Dassuncao, C., Tokranov, A. K., Wagner, C. C., and Allen, J. G. (2019). A review of the pathways of human exposure to poly- and perfluoroalkyl substances (PFASs) and present understanding of health effects. *J. Expo. Sci. Environ. Epidemiol.* **29**, 131–147. 10.1038/s41370-018-0094-1.

Tawe, W. N., Eschbach, M. L., Walter, R. D., and Henkle-Duhrsen, K. (1998). Identification of stress-responsive genes in *Caenorhabditis elegans* using RT-PCR differential display. *Nucleic Acids Res.* **26**, 1621–1627.

Tieu, K., Perier, C., Caspersen, C., Teismann, P., Wu, D. C., Yan, S. D., Naini, A., Vila, M., Jackson-Lewis, V., Ramasamy, R., *et al.* (2003). D-Beta-hydroxybutyrate rescues mitochondrial respiration and mitigates features of Parkinson disease. *J. Clin. Investig.* **112**, 892–901.

USEPA (2017). *Technical Fact Sheet—Perfluorooctane Sulfonate (PFOS) and Perfluorooctanoic Acid (PFOA) At a Glancelevel*. https://www.epa.gov/sites/production/files/2017-12/documents/ffrrofact-sheet_contaminants_pfos_pfoa_11-20-17_508_0.pdf

USEPA (2019). *Drinking Water Health Advisories for PFOA and PFOS*. https://www.epa.gov/ground-water-and-drinking-water/drinking-water-health-advisories-pfoa-and-pfos

Vanfleteren, J. R. (1993). Oxidative stress and ageing in *Caenorhabditis elegans*. *Biochem. J.* **292**(Pt 2), 605–608.

Weiss-Errico, M. J., Miksovska, J., and O'Shea, K. E. (2018). Beta-cyclodextrin reverses binding of perfluorooctanoic acid to human serum albumin. *Chem. Res. Toxicol.* **31**, 277–284.

Weiss-Errico, M. J., and O'Shea, K. E. (2017). Detailed NMR investigation of cyclodextrin-perfluorinated surfactant interactions in aqueous media. *J. Hazard. Mater.* **329**, 57–65.

Wenz, C., Faust, D., Linz, B., Turmann, C., Nikolova, T., Bertin, J., Gough, P., Wipf, P., Schroder, A. S., Krautwald, S., *et al.* (2018). t-BuOOH induces ferroptosis in human and murine cell lines. *Arch. Toxicol.* **92**, 759–775.

Xu, T., Li, P., Wu, S., Li, D., Wu, J., Raley-Susman, K. M., and He, D. (2016). Chronic exposure to perfluorooctane sulfonate reduces lifespan of *Caenorhabditis elegans* through insulin/IGF-1 signaling. *Bull. Environ. Contam. Toxicol.* **97**, 119–123.

Xun, Z., Rivera-Sanchez, S., Ayala-Pena, S., Lim, J., Budworth, H., Skoda, E. M., Robbins, P. D., Niedernhofer, L. J., Wipf, P., and McMurray, C. T. (2012). Targeting of XJB-5-131 to mitochondria suppresses oxidative DNA damage and motor decline in a mouse model of Huntington's disease. *Cell Rep.* **2**, 1137–1142.

Yao, C., El Khoury, R., Wang, W., Byrd, T. A., Pehek, E. A., Thacker, C., Zhu, X., Smith, M. A., Wilson-Delfosse, A. L., and Chen, S. G. (2010). LRRK2-mediated neurodegeneration and dysfunction of dopaminergic neurons in a *Caenorhabditis elegans* model of Parkinson's disease. *Neurobiol. Dis.* **40**, 73–81.

Young, A. B. (2009). Four decades of neurodegenerative disease research: How far we have come! *J. Neurosci.* **29**, 12722–12728.